© 2018. Published by The Company of Biologists Ltd | Journal of Cell Science (2018) 131, jcs219014. doi:10.1242/jcs.219014

CORRECTION

Correction: Secretion of ERP57 is important for extracellular matrix accumulation and progression of renal fibrosis, and is an early sign of disease onset (doi:10.1242/jcs.125088)

Hassan Dihazi, Gry Helene Dihazi, Asima Bibi, Marwa Eltoweissy, Claudia A. Mueller, Abdul R. Asif, Diana Rubel, Radovan Vasko[1] and Gerhard A. Mueller

There was an error published in *J. Cell Sci.* (2013) **126**, 3649–3663 (doi:10.1242/jcs.125088).

The affiliations for Marwa Eltoweissy were incorrect. The correct affiliations are as given below.

Hassan Dihazi[1], Gry Helene Dihazi[1], Asima Bibi[1], Marwa Eltoweissy[1,2], Claudia A. Mueller[3], Abdul R. Asif[4], Diana Rubel[1], Radovan Vasko[1] and Gerhard A. Mueller[1]

[1]Department of Nephrology and Rheumatology, Georg-August University Goettingen, Robert-Koch-Strasse 40, 37075 Goettingen, Germany. [2]Department of Zoology, Faculty of Science, Alexandria University, Alexandria, Egypt. [3]Section for Transplantation, Immunology and Immunohematology, ZMF, Eberhard-Karls-University Tuebingen, Germany. [4]Department of Clinical Chemistry, Georg-August University Goettingen, Goettingen, Germany

Marwa Eltoweissy apologises to the readers for any confusion that this error might have caused.

Secretion of ERP57 is important for extracellular matrix accumulation and progression of renal fibrosis, and is an early sign of disease onset

Hassan Dihazi[1,*], Gry Helene Dihazi[1], Asima Bibi[1], Marwa Eltoweissy[1], Claudia A. Mueller[2], Abdul R. Asif[3], Diana Rubel[1], Radovan Vasko[1] and Gerhard A. Mueller[1]

[1]Department of Nephrology and Rheumatology, Georg-August University Goettingen, Robert-Koch-Strasse 40, 37075 Goettingen, Germany
[2]Section for Transplantation, Immunology and Immunohematology, ZMF, Eberhard-Karls-University Tuebingen, Germany
[3]Department of Clinical Chemistry, Georg-August University Goettingen, Goettingen, Germany

*Author for correspondence (dihazi@med.uni-goettingen.de)

Accepted 20 May 2013
Journal of Cell Science 126, 3649–3663

doi: 10.1242/jcs.125088

Summary

Renal fibrosis is characterized by excessive accumulation of extracellular matrix (ECM), which compromises organ function by replacing normal organ tissue. The molecular mechanisms leading to renal fibrosis are not fully understood. Here we demonstrated that TGFβ1, AGT or PDGF stimulation of renal cells resulted in endoplasmic reticulum (ER) stress followed by activation of the protective unfolded protein response pathway and a high secretory level of protein disulfide isomerase ERP57 (also known as PDIA3). The TGFβ1-induced impairment of ER function could be reversed by treatment with BMP7, suggesting a specific involvement in renal fibrosis. A clear correlation between the degree of fibrosis, ER stress and the level of ERP57 could be seen in fibrosis animal models and in biopsies of renal fibrosis patients. Protein interaction studies revealed that secreted ERP57 exhibits a strong interaction with ECM proteins. Knockdown of ERP57 or antibody-targeted inhibition of the secreted form significantly impaired the secretion and accumulation of ECM. Moreover, ERP57 was excreted in the early stages of chronic kidney disease, and its level in urine correlated with the degree of renal fibrosis, suggesting that the secretion of ERP57 represents one of the first signs of renal fibrosis onset and progression.

Key words: ECM, *ERP57*, ER stress, Renal fibrosis, UPR

Introduction

Renal diseases are rapidly increasing in western populations due to a continuous rise of common illnesses such as diabetes mellitus and hypertension. Numerous risk factors (e.g. inflammation, elevated arterial blood pressure, hyperglycemia, proteinuria, toxins, drugs, hypoxia and hyperfiltration) are known to induce renal diseases, which often lead to endstage renal failure (ERF) through a common pathway of renal fibrosis. Until now, diagnostic tools for the early recognition of renal failure as a major risk factor of ERF in the clinical settings are insufficiently developed. Also, discrimination of irreversibly progredient renal diseases from occasionally observed reversible damages are not defined. There is still an incomplete understanding of the process of renal failure in addition to a lack of effective preventative therapy. Renal failure is a process that is characterized by the excessive accumulation of extracellular matrix (ECM) deposition in the tubulo-interstitial space and is associated with declining excretory renal function (Hirschberg, 2005). The molecular mechanisms of fibrosis are not fully understood, but imbalance of ECM synthesis and degradation was described as a common final pathway. In healthy kidney, the formation of ECM and its degradation are in homeoestatic equilibrium, whereas in fibrotic kidney this balance is disturbed owing to a high rate of ECM synthesis and a low level of its degradation or to a combination of both (Branton and Kopp, 1999; Eitner and Floege, 2005; Liu, 2006). It appears to result from pathological, dysregulated repair mechanisms of diverse renal injuries within the interstitial space. Interstitial renal fibroblasts at different stages of differentiation are key players in this process. Like in wound healing, different cytokines (e.g. TGFβ1 and BMP7) and enzymes [e.g. matrix metallo-proteases (MMPs)] that regulate tissue remodelling seem to be involved. New insights into renal failure suggest that this process is related to complex local interactions of cells of the interstitial and vascular space as well as interactions of tubuli, but also correlates in part with cellular feeding from blood-borne progenitor cells (Harris and Neilson, 2006; Iwano and Neilson, 2004). Genetic factors predisposing to renal failure might be relevant for specific external or internal deteriorating stimuli, such as in diabetic nephropathy. At present, the relative importance of each of these components in the development of renal failure or in physiological renal repair is still unknown. Among the mechanisms involved in renal failure, stress pathways were reported to inhibit ECM degradation through upregulation of the plasminogen activator inhibitor-1 system (PAI-1), which has an important function in modulating the degradation of ECM (Lassila et al., 2007; Lee et al., 2005; Nangaku, 2006). Despite the progress reported in this field (Djamali, 2007; Iwano and Neilson, 2004; Qi et al., 2006), the mechanisms leading to renal fibrosis still remain poorly understood.

The knowledge of molecular mechanisms involved in ECM turnover might contribute to a better understanding of the pathological process to improve therapeutic strategies. Like all proteins destined for secretion, ECM proteins are translocated into the endoplasmic reticulum (ER) where folding takes place before secretion through the Golgi complex. Because of the high protein concentration in the ER, lumen cells express molecular chaperones to assist folding by blocking nonspecific intermolecular interactions, in particular aggregation (Bedard et al., 2005; Hebert and Molinari, 2007). The levels of the chaperons are continuously adjusted to cope with stress conditions and to satisfy the needs of the cell (Dobson, 2003; Goldberg, 2003). An overload of ER with nascent proteins results in ER stress and activation of the unfolded protein response (UPR) pathway, leading to upregulation of ER-stress proteins to improve the folding procedure. ER stress has been linked to a large number of diseases including cancer, diabetes, cardiac disease and muscle degeneration (Oyadomari and Mori, 2004). The investigation of the mechanisms connecting ER stress to the pathophysiology of renal fibrosis is of great interest in order to explore the potential of key proteins of this pathway in drug discovery and therapeutic aspects.

In the present study, we performed functional proteomics of model cell lines to identify new pathways involved in renal fibrosis. We demonstrate a strong involvement of ER-stress proteins in the synthesis and secretion of ECM. Moreover, we identify ERP57 (also known as PDIA3) as key protein in ECM protein synthesis and accumulation, and present it as a potential diagnostic marker for renal fibrosis and therapeutic target.

Results

TGFβ1-induced cell transformation impacts the renal cell proteome

Despite the complex molecular mechanisms involved in renal failure, one of the central regulators of tissue fibrosis is the cytokine transforming growth factor-beta (TGFβ), including at least three highly homologous mammalian isoforms TGFβ1, 2 and 3, which have similar profibrogenic effects *in vitro*. Also *in vivo*, the profibrotic effect of TGFβ1 is well established, because it is overexpressed in most fibrotic tissues. Furthermore, TGFβ1 transgenic mice develop progressive fibrosis in multiple organs, especially the kidneys. In order to identify new molecular factors and pathways potentially associated with renal failure at the cellular level, we used cell models with established inducible profibrogenic phenotypes (Bechtel et al., 2010; Zeisberg et al., 2005). For this purpose, cell extracts were prepared from the control and from the TGFβ1-treated renal fibroblast cell line TK173 (72 h). Proteins were separated by two-dimensional gel electrophoresis (2-DE). The protein expression patterns from the two cell extracts were compared with each other using the Delta2D software (Decodon GmbH). Two-dimensional protein maps derived from the cell extracts analyzed with conventional 2-DE in the pH ranges 3–10 and 5–8 identified more than 2350 protein spots in each analysed cell extract when 20,000 pixels were used as the filter limit. The pixel volume of each spot provides the basis for comparison of the protein expression patterns between control and TGFβ1-treated TK173 cells. A representative 2-DE protein map from TGFβ1-treated TK173 for pH 5–8 is shown in supplementary material Fig. S1A,B. To ensure solid quantification of differentially expressed proteins, 2D-difference gel electrophoresis (DIGE) analysis was performed with the two cell extracts using Cydyes, as described in Materials and Methods. The 2D-DIGE images were analyzed using the Delta2D software (Decodon); interesting protein spots were excised and analyzed by mass spectrometry. The proteins were identified using the MASCOT Database. A total of 114 differentially expressed proteins were identified (supplementary material Table S1). Comparing the treated cells with the control revealed that treatment with TGFβ1 resulted in the alteration of 62 non-redundant proteins ($P<0.05$). Among these proteins, 13 were found to be downregulated (Table 1), whereas 49 were upregulated (Table 2). The identified proteins were found to be associated with different biological functions and a large number of them could be classified into three functional categories: the first category grouped the proteins that are known to be involved in fibrogenesis (COL1A1, FIN, ACTA2, VIN, VIM, DES), confirming a profibrotic effect of the cytokine TGFβ1 on TK173. The other two categories involved protein markers of the ER stress- and the UPR (unfolded protein response)-pathways (GRP78, GRP94, ERP57, ERP72 and CALR) (Fig. 1A–C), and proteins of the oxidative stress pathway (PRDX1, PRDX2, PRDX6, SOD2, PARK7, HYOU1), which were highly upregulated in TGFβ-treated TK173 cells (Fig. 1A–C).

Upregulation of ER-stress proteins as a cell response to cytokine-induced transformation

To further determine whether the profibrotic cell phenotype with the continuous presence of TGFß1 could be accompanied by the

Table 1. List of proteins found to be downregulated in the TGFβ1-treated TK173 cell line compared with untreated controls

Protein name	Gene symbol	Swiss Prot Acc. No.	Mass	PMF	MS/MS score
Low molecular weight phosphotyrosine protein phosphatase	*ACP1*	P24666	18,031		103
Chloride intracellular channel protein 1	*CLIC1*	O00299	26,906		98
Cystatin-B	*CSTB*	P04080	11,133		92
Eukaryotic translation initiation factor 1	*EIF1*	P41567	12,725		78
Histidine triad nucleotide-binding protein 1	*HINT1*	P49773	13,793		45
Inosine-5′-monophosphate dehydrogenase 2	*IMPDH2*	P12268	55,770		42
NADH dehydrogenase [ubiquinone] flavoprotein 2, mitochondrial	*NDUFV2*	P19404	27,374		109
PEST proteolytic signal-containing nuclear protein	*PCNP*	Q8WW12	18,913		96
Peptidyl-prolyl cis-trans isomerase A	*PPIA*	P62937	18,001		123
Pyruvate kinase isozymes M1/M2	*PKM2*	P14618	57,937		145
Splicing factor, arginine/serine-rich 1	*SFRS1*	Q07955	27,728	96	
Tubulin-specific chaperone A	*TBCA*	O75347	12,847		89
Ubiquitin-conjugating enzyme E2 N	*UBE2N*	P61088	17,127	141	

The accession number in Swiss-Prot, the peptide mass fingerprinting (PMF) and MS/MS information are given. The spots where MS/MS-data are missing were only identified with PMF.

Table 2. List of proteins found to be upregulated in the TGFβ1-treated TK173 cell line compared with untreated control cultures

Protein name	Gene symbol	Swiss Prot Acc. No.	Mass	PMF	MS/MS score
Actin, aortic smooth muscle	*ACTA2*	P62736	42,009		152
Actin, cytoplasmic 1	*ACTB*	P60709	41,710		117
Actin, cytoplasmic 2	*ACTG1*	P63261	41,766		214
Alpha-actinin-1	*ACTN1*	P12814	102,993		110
BAG family molecular chaperone regulator 2	*BAG2*	Q95816	23,757		60
UPF0568 protein C14orf166	*C14orf166*	Q9Y224	28,068	81	
Caldesmon	*CALD1*	Q05682	93,194		173
Calreticulin	*CALR*	P27797	48,142		210
Caprin-1	*CAPRIN1*	Q14444	78,318		122
Calponin-2	*CNN2*	Q99439	33,675		70
CNN2 protein	*CNN2*	Q6FHE4	33,709	151	
Collagen alpha-1(I) chain	*COL1A1*	P02452	138,941		251
Desmin	*DES*	P17661	53,536		132
Endoplasmic reticulum resident protein 29	*ERP29*	P30040	28,993		95
Protein disulfide-isomerase	*ERP57*	P30101	56,747		213
Protein disulfide-isomerase A4	*ERP72*	P13667	72,932		165
Fatty acid-binding protein, epidermal	*FABP5*	Q01469	15,164		78
Fibronectin	*FN1*	P02751	262,442		157
Endoplasmin	*GRP94*	P14625	92,411		231
Glutathione S-transferase P	*GSTP1*	P09211	23,341		187
Histone H2B type 1-B	*HIST1H2BB*	P33778	13,942		209
Heterogeneous nuclear ribonucleoprotein A/B	*HNRNPAB*	Q99729	36,225		125
Heterogeneous nuclear ribonucleoprotein H	*HNRNPH1*	P31943	49,229		105
Heterogeneous nuclear ribonucleoprotein H3	*HNRNPH3*	P31942	36,926		105
Heterogeneous nuclear ribonucleoprotein K	*HNRNPK*	P61978	50,944		229
Heterogeneous nuclear ribonucleoprotein D-like	*HNRPDL*	O14979	46,438	89	
78 kDa glucose-regulated protein	*HSPA5*	P11021	72,288		395
Hypoxia upregulated protein 1	*HYOU1*	Q61N67	111,266		416
LIM and SH3 domain protein 1	*LASP1*	Q14847	29,717		98
Galectin 1	*LGALS1*	P09382	14,706		157
Protein DJ-1	*PARK7*	Q99497	19,891		135
Protein disulfide-isomerase	*PDI*	P07237	57,116		133
Peroxiredoxin-1	*PRDX1*	Q06830	22,110		96
Peroxiredoxin-2	*PRDX2*	P32119	21,892		158
Thioredoxin-dependent peroxide reductase, mitochondrial	*PRDX3*	P30048	27,675		218
Peroxiredoxin-6	*PRDX6*	P30041	25,035		215
Proteasome subunit beta type-6	*PSMB6*	P28072	25,341		119
GTP-binding nuclear protein Ran	*RAN*	P62826	24,423		92
RNA-binding protein 8A	*RBM8A*	Q9Y5S9	19,877		151
40S ribosomal protein S12	*RPS12*	P25398	14,515	88	
Superoxide dismutase [Cu-Zn]	*SOD1*	P00441	15,936		112
Superoxide dismutase [Mn], mitochondrial	*SOD2*	P04179	24,722		154
Triosephosphate isomerase	*TPI1*	P60174	26,653		127
Tubulin alpha-1A chain	*TUBA1A*	Q71036	50,104		121
Tubulin alpha-1C chain	*TUBA1C*	Q9BQE3	49,863	198	
Thioredoxin	*TXN*	P10599	11,730		168
Vinculin	*VCL*	P18206	123,799		98
Transitional endoplasmic reticulum ATPase	*VCP*	P55072	89,266		210
Vimentin	*VIM*	P08670	53,619		340

The accession number in Swiss-Prot, the peptide mass fingerprinting (PMF) and MS/MS information are given. The spots where MS/MS-data are missing were only identified with PMF.

activation of UPR and alteration in the expression of the ER-stress proteins at the cellular level, TK173 as model system was stimulated for different periods of time with the profibrotic cytokine TGFβ1, and the expression of the proteins of interest was analysed by western blot analysis and immunofluorescence staining. The activation of TK173 into a profibrotic phenotype upon treatment with TGFβ1 was accompanied by a progressive and time-dependent upregulation of the ER-stress proteins (GRP78, GRP94, ERP57, ERP72, and CALR) (Fig. 1D). In parallel to the increase in ER-stress protein expression, a substantial and progressive upregulation in fibrosis and myofibroblast markers (e.g. FIN, ACTA2, VIM, DES) expression and secretion was confirmed in cell extracts and supernatants, respectively (Fig. 1E,F). The extensive upregulation of ER-stress proteins was observed in the first week of treatment. Long-term exposure to TGFβ1 resulted in cell adaptation and regeneration of normal levels of ER-stress proteins but not of the fibrosis markers, indicating a persistent cell alteration. The profibrotic effects of TGFβ1 on the fibroblast cell line TK173 were accompanied by a progressive increase in the expression of the key proteins of ER-stress protein. Western blot and immunofluorescence data strengthened the proteomics results and suggested an important role of the UPR pathway and ER-stress proteins in TGFβ1 signalling and in the pathogenesis of renal fibrosis.

Upregulation of ER-stress proteins and activation of the UPR pathway play an important role in renal fibrosis

To ensure that activation of UPR and the alteration in expression of ER-stress proteins is not restricted to TGFβ1 and activated renal

fibroblasts, two renal cell lines derived from different parts of the kidney (from interstitial part the TK173 and from proximal Tubule HK-2) were treated with three different profibrotic cytokines (*TGFβ1*, *AGT* and *PDGF*) for 72 h. The expression of the protein of interest was investigated using western blot analysis. A substantial upregulation of CALR, GRP78, ERP57 and ERP72

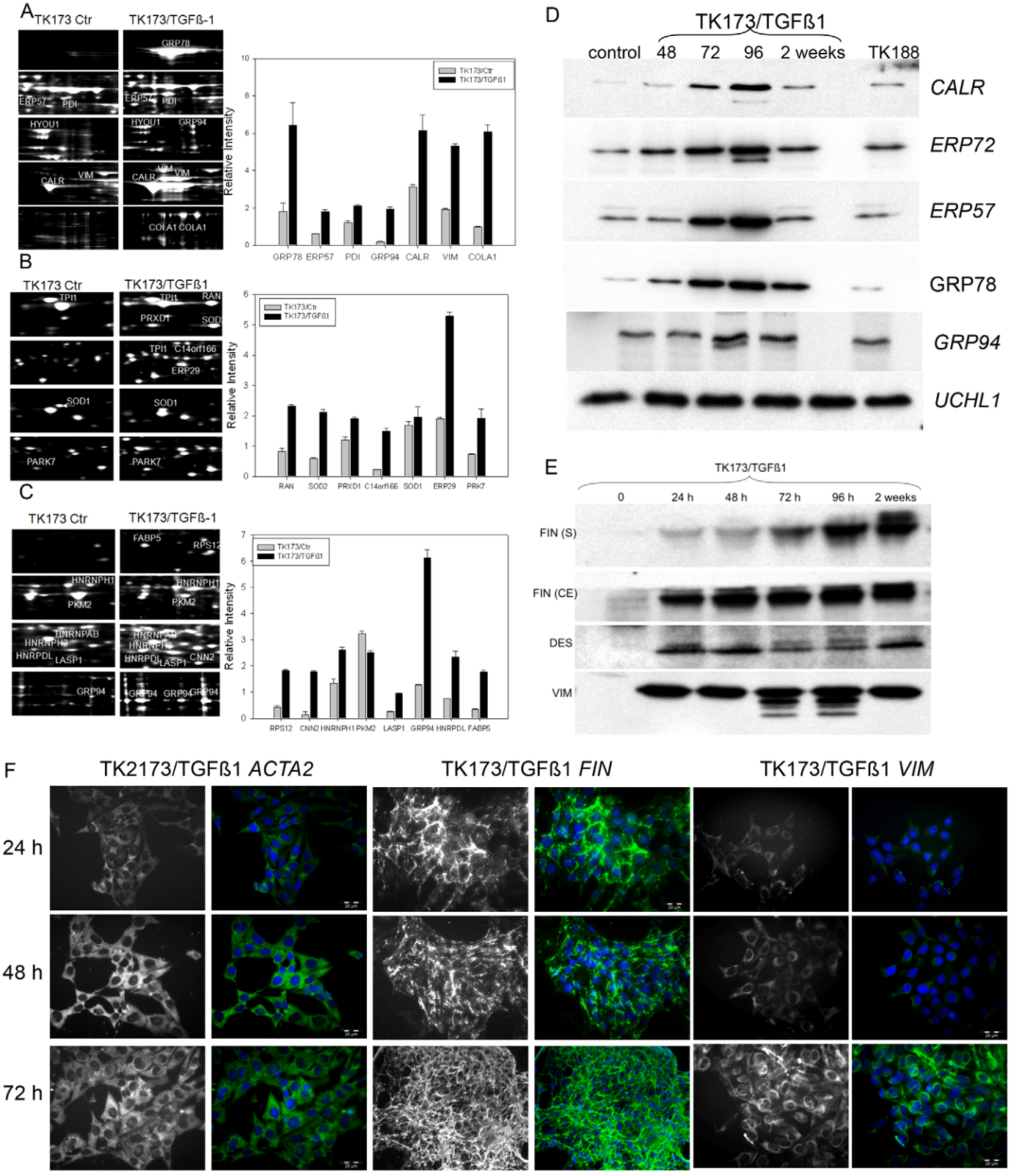

Fig. 1. See next page for legend.

was observed in renal cells treated with the three cytokines. Moreover, overexpression of CHOP and EIF2A together with increased levels of phosphorylated EIF2A were detected under all three treatments (Fig. 2A,B). To ensure the involvement of the UPR pathway in fibrosis, activation of UPR-key proteins PERK, IREa1 and ATF6 was investigated in renal cell lines treated with TGFβ1, tunicymycin and thapsigargin. In a similar manner to tunicamycin, IREa1 and PERK were phosphorylated upon treatment with TGFβ1. Moreover, activation of ATF6, as shown by the cleaved form, was observed in tunicamycin and TGFβ1-treated cells (Fig. 2C). The phosphorylation of IREa1 and PERK, and the cleavage of ATF6 suggest that the UPR pathway activation and the subsequent alteration in the expression of ER-stress proteins are common pathways in the progression of renal fibrosis. Our suggestion was supported by the fact that treatment with BMP7, a TGFβ1 antagonist, significantly reversed the TGFβ1-induced ER-stress and activation of the UPR pathway (Fig. 2D,E).

The induction of ER-stress proteins is proportional to the progression of renal fibrosis

To investigate the involvement of ER-stress proteins in renal fibrosis, the *Col4a3* knockout mouse, an animal model for chronic progressive renal fibrosis, was used. Animals from different stages of the disease (4, 6, 7 and 9 weeks) were killed and the kidneys were harvested. After lysis of the kidneys and preparation of the protein extracts, the changes of the ER-stress protein expression were monitored by western blot analysis. Parallel to the progression of renal fibrosis (Fig. 3A), there was a significant increase in ER-stress and UPR revealed by the increase in expression of the ER-stress proteins (Fig. 3B).

ERP57 is secreted into the extracellular medium upon cytokine treatment

The results presented above point to an involvement of ER-stress proteins in renal fibrosis. These proteins also have an important role in the folding of secretory proteins (e.g. ECM). Besides its chaperone function, the protein disulfide isomerase ERP57 catalyses the formation and breakage of disulfide bridges, which are often vital for the stability of the final protein structure. The incorrect pairing of cysteine residues usually prevents the folding of a protein into its native conformation and leads to its degradation (Ahamed et al., 2006). The formation of biosynthetic disulfide bonds is an important step in the maturation of ECM proteins (COL1A1, FIN and LAMN) in eukaryotic cells. The preservation of the protein conformation and the disulfide bridges is crucial for the accumulation of ECM in the extracellular milieu. Secreted proteins are exposed to a highly reducing extracellular environment, often leading to impairment of the disulfide bridges and destruction of the ECM network. We hypothesized that, in case of renal fibrosis, the maintenance of stable ECM and its protection from the reducing extracellular environment requires the involvement of secretory protecting proteins, and that this process is regulated by profibrotic cytokines. To prove our assumption we investigated whether treatment with profibrotic cytokines can cause the secretion of folding proteins. TK173 and HK-2 cells were cultured in FCS-free medium for 24 h. Subsequently, the cells were treated with TGFβ1, PDGF or AGT for 24 h. Control cells were incubated in FCS-free medium without treatment. The medium with the cytokines was changed to avoid any minimal impact of dead cells on the supernatant proteome, and the cells were incubated for an additional 48 h with the three cytokines separately. The supernatant (with almost no dead cells) was collected and the proteins were extracted, as described in Materials and Methods, and analyzed by 2-DE. Surprisingly, the image analysis and identification by mass spectrometry of the proteins showed that among the ER-stress protein *ERP57* was secreted in higher amounts in both cell lines under all three treatment conditions, suggesting a potential function in ECM stabilization (Fig. 4A,B). Moreover, our 2D gels revealed that compared with the cytosolic form, the excreted ERP57 protein exhibited post-translational modifications as shown by the presence of several spots (up to five) with different pIs on 2-D gels (Fig. 4A,B).

To ensure that the secretory effect of ERP57 is correlated to a profibrotic phenotype, renal cells were treated with tunicamycin, an antibiotic that blocks the first step of glycoprotein synthesis and activates the UPR pathway leading to ER stress. In a similar manner to TGFβ1, treatment with tunicamycin resulted in upregulation of ERP57 (Fig. 4Ci,ii). In contrast to TGFβ1, the protein was not detected in the supernatant of cells treated with tunicamycin, confirming that ER stress and activation of the UPR-pathway do not automatically result in secretion of ERP57 (Fig. 4D). This confirms that the secretion of ERP57 upon treatment with TGFβ1 is not the result of only ER-stress and UPR-pathway activation.

Excretion of ERP57 in urine as an early diagnostic marker for renal fibrosis

The stimulated renal cells react by secreting ERP57 upon cytokine treatment. This response can be one of the first signs of fibrosis, and if so, the protein has the potential to be an earlier marker for renal fibrosis. To investigate our hypothesis and to prove the usefulness of the secreted ERP57 as a marker for renal fibrosis, urine samples from 15 diabetic patients with lower microalbuminuria (20–50 mg/l), 15 urine samples from AKI patients and 15 samples from healthy controls were collected. After protein precipitation and estimation, the ERP57 excretion levels in urine were quantified using western blot analysis. The immunoblot data could clearly confirm the exclusive excretion of ERP57 in diabetic patients in the earlier stages of nephropathy

Fig. 1. TGFβ1 induces ER-stress and cell transformation towards the fibrosis phenotype. (**A–C**) Graphs represent enlargement of the gel regions of interest showing protein spots found to be differentially expressed under treatment with TGFβ1. The quantification of protein expression in the TK173 cell line for selected proteins is given in the form of bar diagrams. On the *y*-axis, the relative intensity of spot is given, on the *x*-axis the corresponding gene name is shown. The quantification of the spots is presented as a grouped bar chart with error bars. Each bar represents the intensity means ± s.d. of protein spots from three independent experiments as quantified by 2D-DIGE using Delt2D software. Significant differences changes upon TGFβ1 treatment: $*P<0.05$, $**P<0.01$, $***P<0.001$. (**D**) Western blot analysis of protein expression changes after TGFβ1 treatment of TK173. The cells were treated for different time periods with TGFβ1, the cell extracts were prepared and the western blot analysis was performed using antibodies against GRP78, GRP94, ERP57, ERP72 and CALR found to be upregulated with 2-DE; UCHL1 was used as control protein for the protein-amount-dependent artefacts. (**E**) The cells were treated for different time periods with TGFβ1. The cell extracts (CE) and supernatants (S) were prepared, and the western blot analysis was performed using antibodies against fibrosis markers such as VIM, DES and FIN. (**F**) Immunofluorescence staining of protein markers of fibrosis (VIM, ACTA2 and FIN) after TGFβ1 treatment. The time-dependent changes in expression were documented.

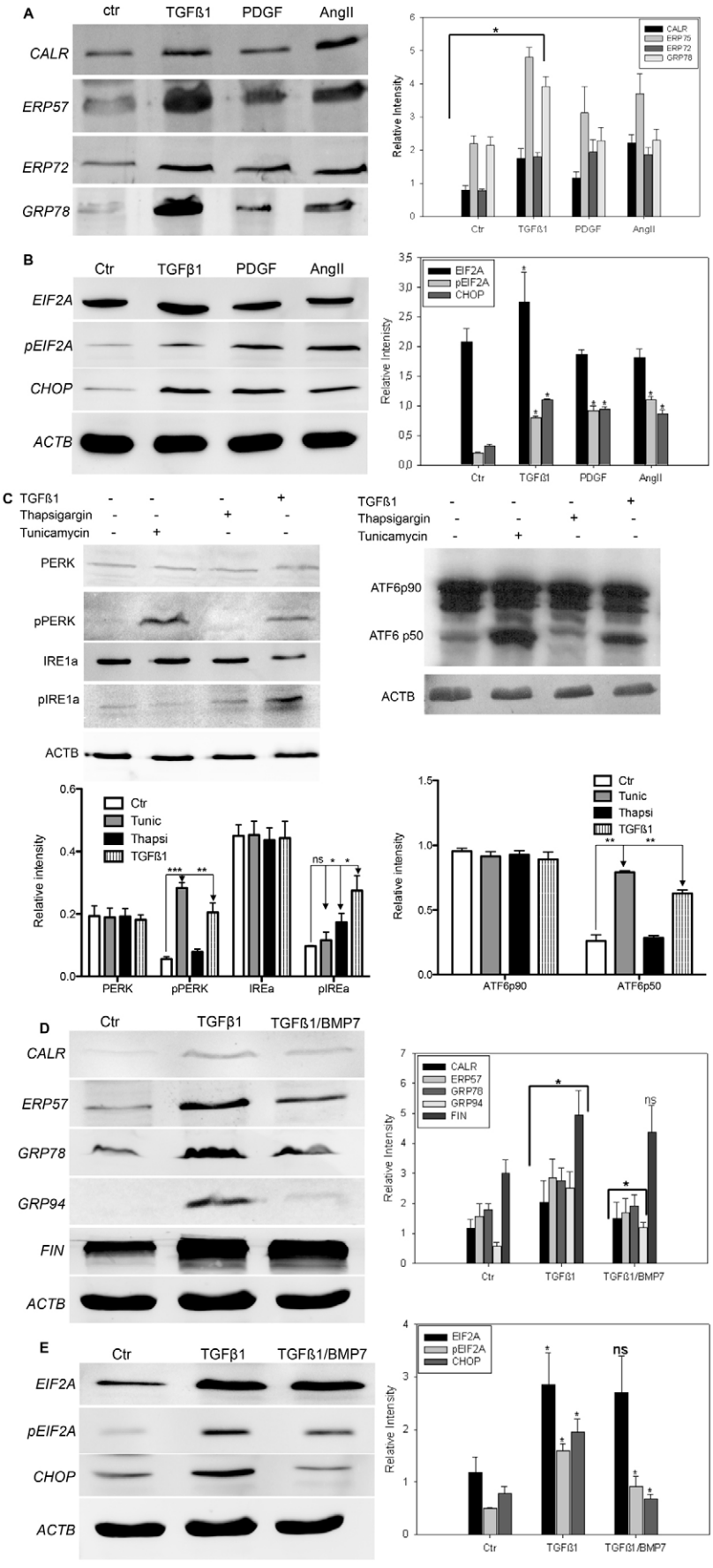

Fig. 2. ER Stress and UPR as common pathways for fibrosis. Western blot analysis of protein expression changes after treatment of renal cells with TGFβ1, PDGF or AGT. The cells were treated for 72 h with one of the cytokines, the cell extracts were prepared and the western blot analysis was performed using antibodies against (**A**) GRP78, ERP57, ERP72 and CALR, and (**B**) EIF2A, phosphorylated EIF2A and CHOP. (**C**) Western blot analysis of the UPR pathway activation. The cells were treated for 72 h with tunicamycin, thapsigargin or TGFβ1, the cell extracts were prepared as described in the Materials and Methods, and western blot analysis was performed using antibodies against IRE1A, phosphorylated IRE1A, PERK, phosphorylated PERK, ATF6 and cleaved ATF6 (**D**,**E**) renal cells were subjected for 48 h to treatment with TGFβ1. A part of the cells was then incubated for additional 72 h with BMP7 (5 ng/ml). Western blot analysis was performed using the antibodies described above. *ACTB* was detected as a protein loading control. The western blot quantification is presented as a grouped bar chart with error bars. Each bar represents the intensity means ± s.d. of blots from three independent experiments. Significant differences: $*P<0.05$, $**P<0.01$, $***P<0.001$.

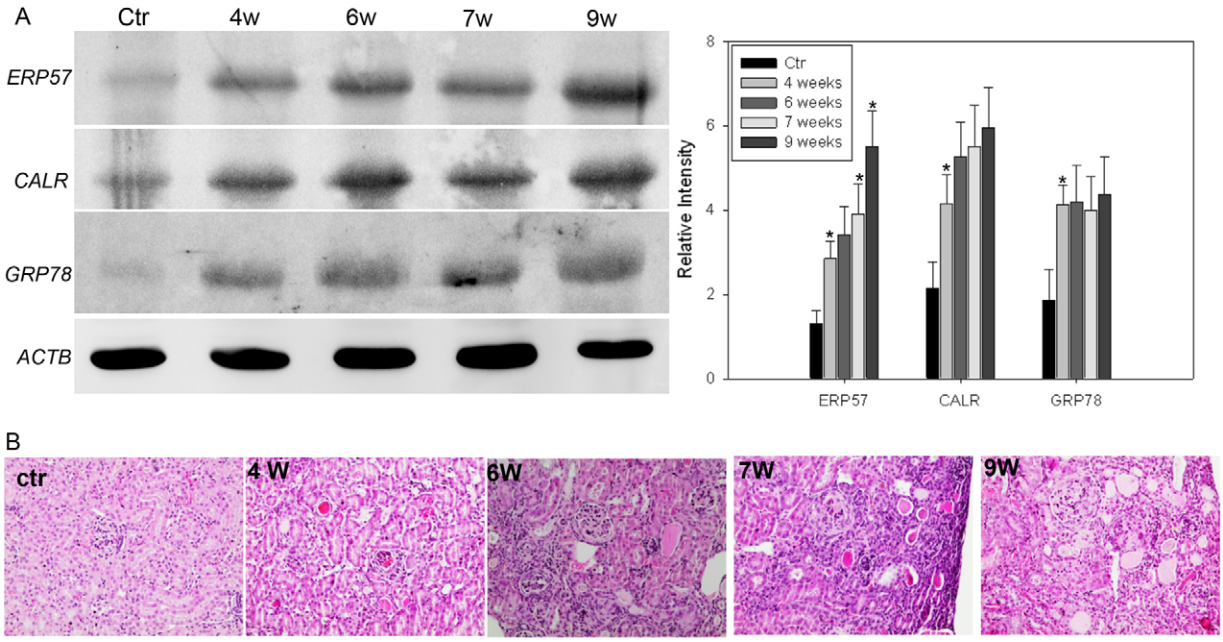

Fig. 3. ER-stress proteins induction is proportional to the renal fibrosis progression. *Col4a3* knockout mice from different stage of the diseases (4, 6, 7 and 9 weeks) were killed and the kidneys were harvested. (**A**) Western blot analysis was performed with the protein extracts. The expression quantification is presented as grouped bar chart. Each bar represents the intensity means ± s.d. of blots from three independent animal groups. ACTB was used as control protein for the protein-amount-dependent artefacts. (**B**) HE staining of kidney from *Col4a3* mice presenting different stages of the disease. The western blot quantification is presented as a grouped bar chart with error bars. Each bar represents the intensity means ± s.d. of blots from three independent experiments. Significant differences: $*P<0.05$, $**P<0.01$, $***P<0.001$.

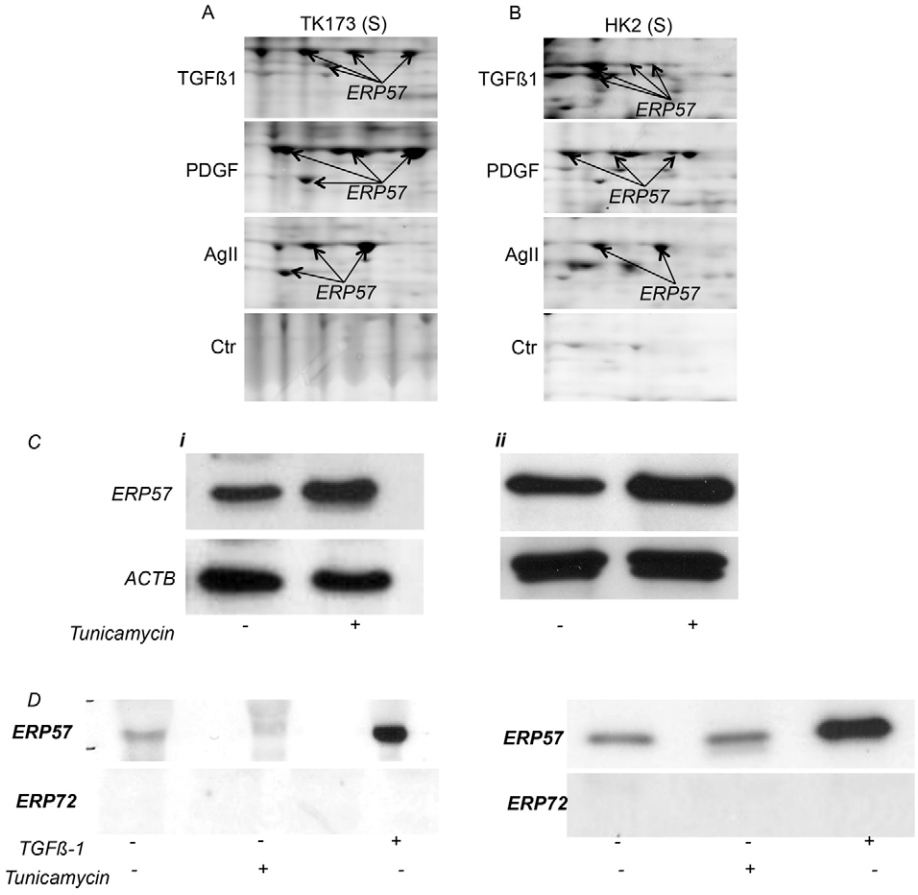

Fig. 4. ERP57 is secreted to extra cellular medium upon cytokine treatment. 2-DE map of cell supernatant after treatment with TGFβ1, PDGF or AGT. TK173 or HK-2 cells were treated for 72 h with one of the cytokines. The proteins were prepared from the supernatant as described in the Materials and Methods, and separated by 2-DE. The protein maps were compared with the control, and the differentially secreted proteins were identified by mass spectrometry. Enlargement of the gel regions of interest showing spots from the secreted ERP57 (**A**) TK173 and (**B**) HK-2. (**C**) Renal cells were treated with tunicamycin and the expression of ERP57 was analyzed by western blot. (**D**) In contrast to TGFβ1, the tunicamycin-induced upregulation of ERP57 did not result in its secretion.

(Fig. 5). The analysis of ERP57 excretion in urine from *Col4a3* knockout mice at different stages of fibrosis clearly confirmed a correlation between the ERP57 excretion level and the progression of renal fibrosis in the first 7 weeks (supplementary material Fig. S2). The decrease in excretion level in later stages could be explained by the relatively higher increase in excretion of plasma proteins (e.g. albumin).

The secreted ERP57 interacts with ECM proteins

To investigate the role of ERP57 in ECM protein folding and stabilization, protein interaction studies were performed. Immunoprecipitation using antibodies against ERP57 or FIN combined with 1D gel and mass spectrometry analysis confirmed a clear interaction between the secreted protein disulfide isomerase ERP57 and ECM proteins, especially FIN and COL1A1 (Fig. 6A–D; supplementary material Tables S2, S3). This suggests an important role of the secreted *ERP57* in ECM stabilization.

Effect of protein disulfide isomerase inhibition on ECM synthesis

To test the effect of protein disulfide isomerase inhibitors on ERP57 secretion and on ECM synthesis and accumulation, TK173 was treated with TGFβ1 supplemented with bacitracin (protein disulfide isomerase inhibitor) and incubated for 72 h. To confirm the inhibition of the enzyme activity, the protein disulfide isomerase activity assay was performed. The activity of the purified recombinant protein disulfide isomerase was compared with its activity in extracts of TK173 cell cultures with and without bacitracin, according to the procedure of Lundström and Holmgren (Lundström and Holmgren, 1990). The time course and concentration of the reduced and precipitated insulin in the TK173 cell extract showed that the increase in disulfide isomerase activity was proportional to the protein concentration and incubation time, as expected (Fig. 7A,B). Moreover, the insulin-reduction assay showed that bacitracin at 200 μM caused a total inhibition of protein disulfide isomerase activity in the TK173 cell extract (Fig. 7C). In contrast to bacitracin, T3 did not significantly reduce the protein disulfide isomerase activity (Fig. 7C). Activity assays performed using anti-ERP57 antibodies, or a combination of anti-ERP57 and anti-ERP72 antibodies as inhibitors, resulted only in partial inhibition of the protein activity in cell extracts (data not shown), indicating the existence of additional protein disulfide isomerases (PDIs) in the analysed cell extracts.

To assess the toxic effect of protein disulfide isomerase inhibitors on TK173 cells, we monitored the response of the cells stimulated with different concentrations of bacitracin and T3 over 24 h using the MTT cell viability assay method. TK173 cells were initially seeded in 96-well plates and grown in normal culture medium. The cells were then stimulated in FCS-free medium with various concentrations of bacitracin or T3 and the percentage viability was compared with an untreated control culture after 24 h and 48 h. As shown in Fig. 7D, cell survival strongly correlated with the concentration of the inhibitors. No significant changes, however, were observed when the incubation time was prolonged. Consequently, experimental conditions for an optimal inhibition of the protein disulfide isomerase experiments over 72 h were designed using concentrations at a maximum of 250 μM in the case of bacitracin and 100 μM in the case of T3.

The effect of the of protein disulfide isomerase inhibition activity on ECM accumulation was then monitored by analysis of the excretion of two components of the ECM, FIN and LAMA1, in the cell culture supernatant of TK173 treated with TGFβ1 combined with either bacitracin or T3. Western blot analysis of the proteins isolated from the supernatants or cell extracts showed a clear decrease in ECM protein synthesis and excretion in cells treated with bacitracin compared with the control and T3 (Fig. 7Eii,iii). Moreover, the expression of ERP57 was also reduced in cells upon treatment with bacitracin, revealing a possible feedback control between the function of ERP57 in the cell and in extracellular medium. Both *in vitro* and *in vivo* experiments showed that T3 had no efficient inhibitory effect on the protein disulfide isomerase activity similar to results reported earlier (Primm and Gilbert, 2001). The impact of ERP57 inhibition on ECM accumulation was also confirmed by specific inhibition with the monoclonal antibody against ERP57. FIN was not able to form dimers as a result of the inhibition of ERP57 (Fig. 7F) and the hindering of disulfide bridge synthesis. These results clearly

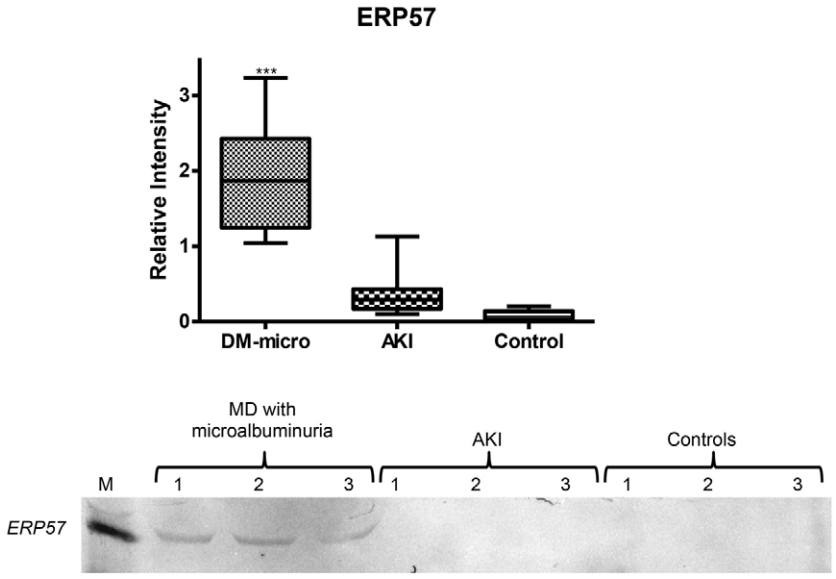

Fig. 5. ERP57 is a potential marker for earlier detection of renal injury. Urine samples from 15 diabetic patients with lower microalbuminuria (20–50 mg/l), 15 urine samples from AKI patients and 15 from healthy controls were collected, and proteins were prepared as described in the Materials and Methods. *ERP57* excretion levels in urine were quantified using western blot analysis. Western blot quantification: on the *y*-axis the relative intensity is given and the *x*-axis shows distribution of the intensity thought the corresponding urine group where the protein was analyzed. The detection of proteins within experimental groups on the blotting membrane was presented below the graph. Statistical analysis was performed using Prizma4 software (***$P<0.001$).

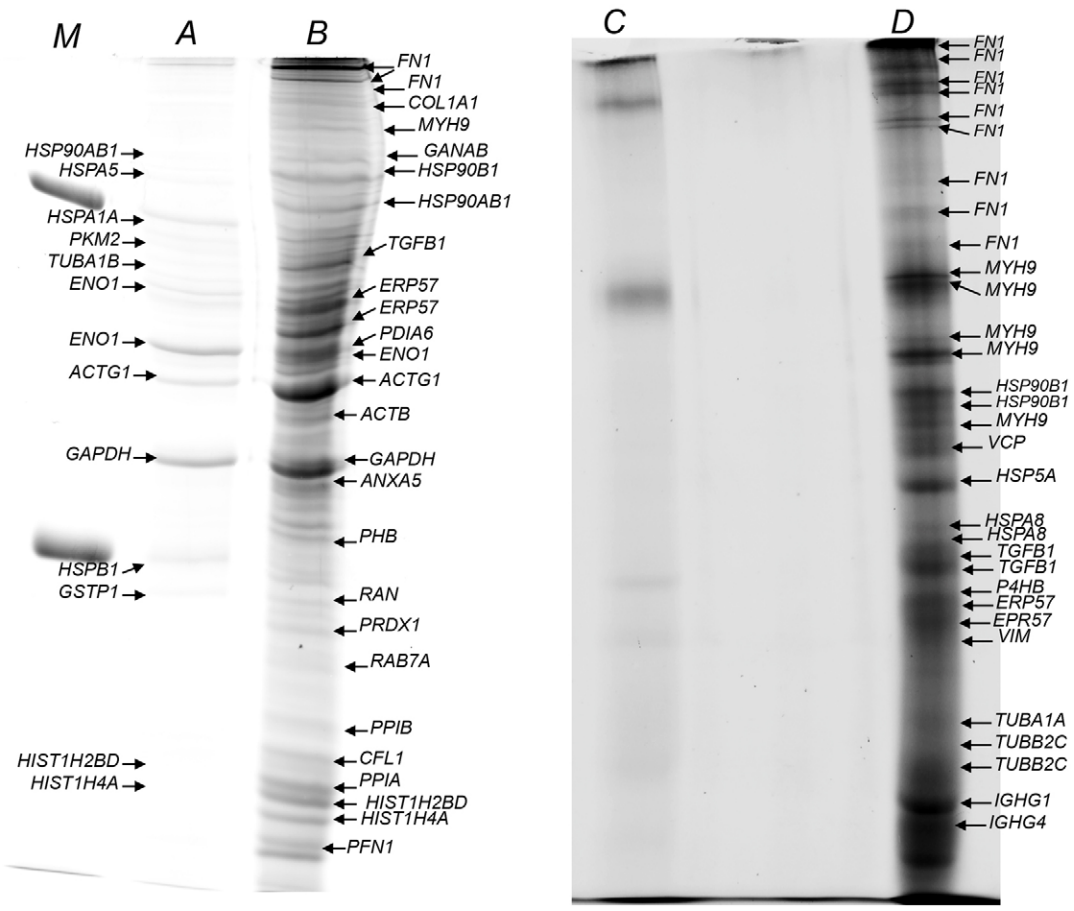

Fig. 6. ERP57 interacts with ECM proteins. Immunoprecipitation (IP) and protein identification using G-protein agarose matrix and antibodies against ERP57 or FIN. ERP57 (**A**,**B**) and FIN (**C**,**D**) were immunoprecipitated with their interaction partners. The resulting proteins were separated using SDS-PAGE and identified using tryptic digestion and mass spectrometry. (A,C) IP using supernatant and G-protein agarose without anti-ERP57 (A) or anti-FIN (B) antibodies. M, protein marker.

demonstrate a pivotal role of ERP57 in EMC protein folding and stabilization.

To support the indispensable role of ERP57 in ECM protein folding and accumulation, we also performed knockdown experiments using siRNA for ERP57 in TK173 cells. Western blot analysis showed an achievement of >90% efficiency in reducing endogenous ERP57 protein levels, whereas β-actin did not show any changes in expression (Fig. 8A). TGFβ1 treatment of knockdown cells did not affect the ERP57 expression level (Fig. 8B). Interestingly, knockdown of ERP57 led to a significant reduction in the ECM protein level, as revealed in the restricted cellular expression of FIN and shown by immunofluorescence staining (Fig. 8C,D). Furthermore, ERP57 knockdown resulted in changes of the cell shape, suggesting an alteration of adhesion proteins as a result of misfolding because of the lack of the appropriate disulfide bridges (Fig. 8D). Similar effects of ERP57 were also detected in cells treated with the reducing agent DTT (Fig. 8D), which confirmed an indispensable role of ERP57 in disulfide-bridge formation and stabilization of ECM proteins.

Discussion

Renal failure is a process characterized by excessive accumulation of ECM deposition in the tubulo-interstitial space, and which is associated with tissue deterioration and a declining excretory renal function (Hirschberg, 2005). The molecular mechanisms of fibrosis are not fully understood, but multiple extracellular stimuli and intracellular signalling pathways (e.g. TGFβ1/Smad signalling) have been implicated, and common pathways of fibrogenesis, such as an imbalance of ECM synthesis and degradation, and cross-linking and stabilization of collagen proteins, have been identified (Branton and Kopp, 1999; Eitner and Floege, 2005; Liu, 2006). Despite the progress reported in this field (Djamali, 2007; Iwano and Neilson, 2004; Qi et al., 2006), the mechanisms leading to renal fibrosis still remain poorly understood. Our study used in the first step functional proteomics to screen potential mechanisms and pathways involved in TGFβ1-induced renal fibrosis, in order to provide further insight into this complex disease. We demonstrate that the stimulation of renal fibroblast or tubular cell lines with cytokines involved in fibrogenesis (e.g. TGFβ1, AGT, PDGF) leads to ER-stress and UPR activation reflected by a substantial overexpression of ER-stress proteins (GRP78, GRP94, ERP57, ERP72, CALR). Alteration in the expression of ER-stress proteins and UPR function has an important role in some human diseases, especially those involving tissues dedicated to extracellular protein synthesis (e.g. insulin in diabetes) (Oyadomari and Mori, 2004). Renal fibrosis is characterized by excess synthesis and secretion of ECM, which leads to a high demand on ER functions with presumed ER

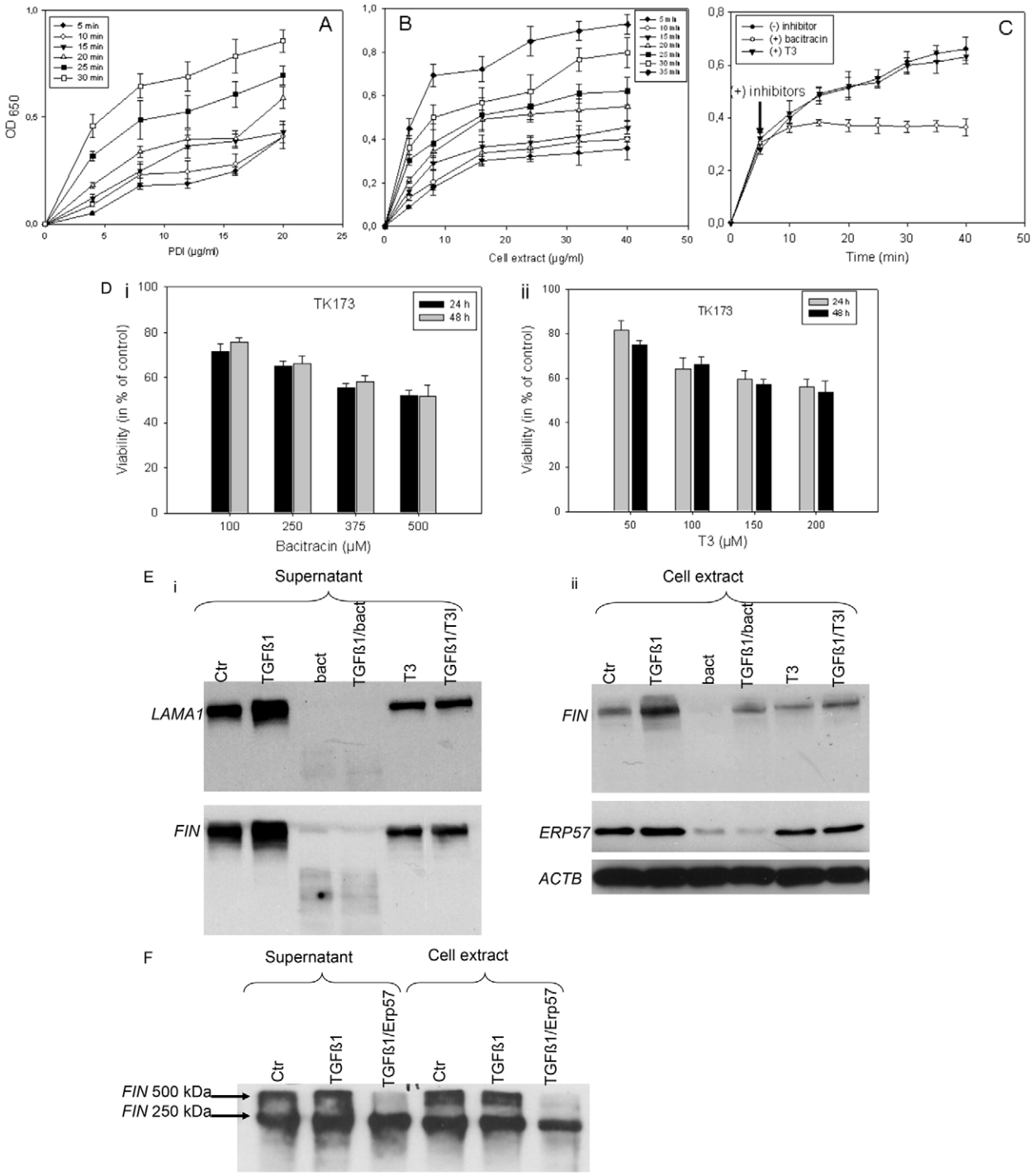

Fig. 7. An alternation in ERP57 expression impairs ECM synthesis and accumulation. Time and concentration course of insulin reduction and precipitation for (**A**) recombinant PDI (0–20 µg/ml) and (**B**) TK173 cell extract. Cell extracts of 4, 8, 16, 24, 32 and 40 µg/ml concentration and GSH were used for insulin reduction. The reaction was followed for each cell extract concentration for 35 min. (**C**) Bacitracin or T3 inhibition of the PDI activity. Reactions were performed using 20 µg cell extract for 40 min, the bacitracin concentration was 250 µM, T3 concentration was 100 µM. Each bar represents the OD650 intensity means ± s.d. of at least three independent experiments. (**D**) The effect of bacitracin and T3 on cell proliferation and viability. TK173 treated with variable bacitracin (100–500 µM) (i) or T3 (50–200 µM) (ii) concentrations for different incubation times and the cell viability was assessed using the MTT [(3-(4,5-dimethylthiazol-2-yl)-2,5-diphenyltetrazolium bromide)] assay. Western blot analyses of ECM components (FIN and laminin) expression and excretion changes in TK173 after TGFβ1 treatment combined either with bacitracin or T3 (**E**) or with anti-*ERP57* antibody. (**F**) The cells were first treated with the inhibitor then with *TGFβ1* (7 ng/ml) for 72 h, the proteins were isolated from cell culture or supernatant as described in Materials and Methods and the western blots were performed with antibodies against FIN and laminin.

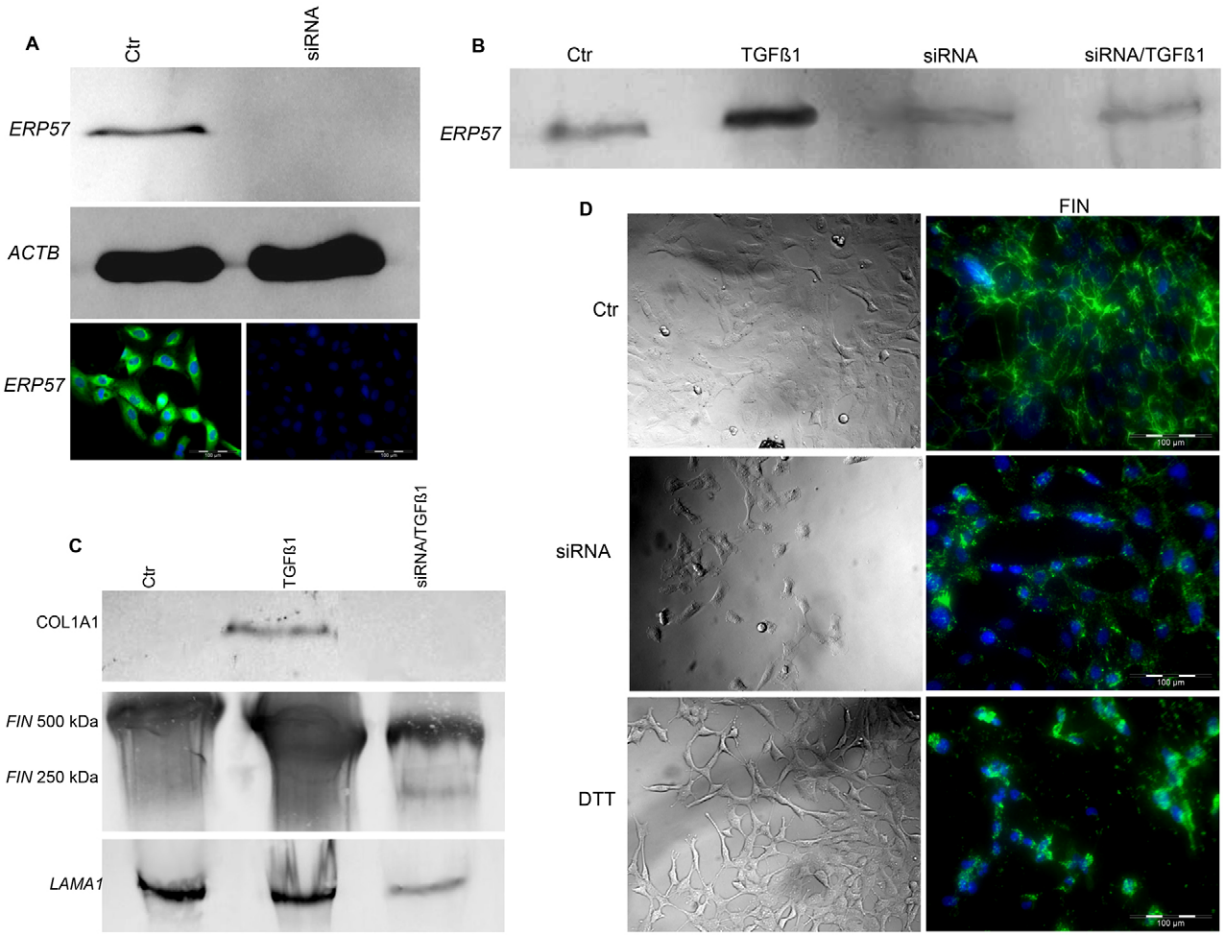

Fig. 8. Downregulation of ERP57 resulted in an alteration in the accumulation of ECM. (**A**) Western blot and immunofluorescence analysis of ERP57 in non-transfected control (Ctr) cells and cells transfected with siRNA vector for ERP57 showing the knockdown of ERP57. (**B**) siRNA-transfected cells and the control were subjected to TGFβ1 stimulation. In contrast to the control, the expression of ERP57 was almost not affected in siRNA-transfected cells. (**C**) siRNA transfected cells showed less ECM expression and accumulation. (**D**) In siRNA cells, FIN expression was restricted to intracellular compartments; FIN accumulation in the extracellular milieu was completely disturbed.

stress and UPR at the cellular level during the course of the disease. The data presented here also suggest a crucial role for ER and ER-stress proteins in ECM synthesis, and thus, most probably in the pathogenesis of renal fibrosis. ER is the site of synthesis and folding of proteins intended to be secreted or displayed on the cell surface (Kim et al., 2008). Important modifications of these secreted proteins, such as glycosylation and disulfide-bond formation, necessitate a special environment outside of the confines of the cytosol. The membranous ER network provides such optimal and isolated conditions to fulfil this function inside the cells. An efficient functioning of the ER is crucial for most cellular activities and survival. Perturbation of ER function results in accumulation and aggregation of unfolded secretory proteins, thus provoking ER stress, which is detected by ER transmembrane receptors and leads to initiation of the UPR to restore normal ER function (Szegezdi et al., 2006). It is well known that stimulation with TGFβ1 activates TGFβ1–Smad signalling, resulting in an increase in the expression of genes encoding proteins involved in renal fibrosis and those that are important for ECM formation such as fibronectins, procollagens and laminins. Our data suggest that the cytokine-activated transcription machinery in renal cells provokes an overloading of the ER with ECM proteins, inducing ER-stress and activating UPR. The UPR attempts to resolve ER stress by inhibiting protein translation, increasing production of chaperone proteins and enhancing protein degradation, allowing the restoration of ER homeostasis and its normal function (Schröder and Kaufman, 2005). To achieve this goal, the UPR stimulates transcription factors, which in turn activate the expression of genes to increase the folding capacity and to improve the ER-assisted degradation (ERAD) (Rao and Bredesen, 2004; Schröder and Kaufman, 2005). We demonstrate that renal cells under cytokine treatment prevent the accumulation of misfolded proteins in the ER by improving the protein folding through the activation of expression of ER chaperones.

Secretory proteins require special post-translational modifications taking place in the ER. Among these modifications, the formation, isomerization and reduction of disulfide bonds are crucial. These modifications are catalyzed by thiol-oxidoreductases of the PDI family. The PDIs are determined by the presence of at least one thioredoxin-like domain with the catalytic activity within the motif CXXC (Frand et al., 2000; Freedman, 1989). ERP57 is a well-characterized member of the PDIs, which forms, breaks and rearranges disulfide bonds in nascent glycoproteins reaching the ER. In the case of ERP57, the redox function is based on the presence of

two active sites of the CGHC (CXXC) motif. The cleavage or formation of the disulfide bond depends on the status of the cysteines in CGHC. The oxidized cysteine forms the disulfide bond, whereas reduced cysteine leads to cleavage of neighboring disulfide bonds. We proved that renal cell lines stimulated with profibotic cytokines increase the expression of ERP57 parallel to their transition to a profibrotic phenotype, as shown by the high expression of fibrosis markers and excretion of a high level of ECM proteins. For the synthesis and correct folding of ECM proteins, especially COL IV, LAMA1/2 and FIN, the disulfide bridges play a crucial role. Without formation of these disulfide bridges, the proteins are misfolded and degraded through the ERAD, which involves the ubiquitin-proteasome system for elimination of unfolded proteins. Upregulation of ERP57 during the progression of renal fibrosis suggests an important role in the formation of disulfide bridges and also protein folding of ECM proteins in the extracellular space. Several interaction partners for ERP57 were identified (Jessop et al., 2007). Among these proteins, laminin and collagen were described as substrates for ERP57. This provides further support that ERP57 directly might interact with EMC proteins in order to form crucial disulfide bridges and to help with the correct folding of these proteins. Downregulation of ERP57 using siRNA has a substantial impact on EMC protein synthesis and secretion. In contrast to other PDIs, ERP57 interacts with the lectins CANX and CALR, and forms a complex, which is part of the glycoprotein-specific quality control machinery operating in the lumen of the ER (Ellgaard and Frickel, 2003). The main target of the complex is to ensure that newly synthesized proteins are correctly folded (Hebert and Molinari, 2007). Overexpression of ERP57 in renal cells upon cytokine treatment might serve to overcome the limiting step in ECM folding to accelerate their proper synthesis and secretion.

It was supposed that because of the KDEL (endoplasmic reticulum retention motif) the PDIs are limited to the ER and the Golgi body (Lewis et al., 1990). However, a number of studies emerged during the last decade, which demonstrated that despite the integrity of the KDEL signal, protein disulfide isomerases can show additional localizations including the Golgi, secretory vesicles and the cell-surface, where they can have an important function in stabilization and the correct folding of secreted proteins (Akagi et al., 1988). The localization and function of PDIs at the cell surface have been proven in a number of investigations including viral fusion and entry (Fenouillet et al., 2001; Markovic et al., 2004; Ryser et al., 1994), gamete fusion (Ellerman et al., 2006), integrin ligation and activation (Lahav et al., 2002; Lahav et al., 2003), inhibition of thrombin generation and fibrin deposition, and initiation of coagulation at sites of vascular damage (Reinhardt et al., 2008; Schott et al., 2005). PDIs of the cell surface and ER are biochemically and immunologically identical, and changes in the expression of intracellular PDIs are mostly reflected in the expression of surface PDIs. ERP57 is the only member of the PDI with a C-terminal motif (QEDL) that seems to be ineffective for ER retrieval (Raykhel et al., 2007), explaining a possible way of escaping the ER retention control. When it is secreted, ECM is exposed to environmental conditions that differ to the highly oxidizing ER environment. This might result in the disruption of disulfide bonds and destabilization of protein structure. We showed that ERP57 was the only member of the PDIs that was found to be secreted in high amounts upon cytokine treatment, even though the renal cells express several other members of the PDI family. Our data suggest that secreted ERP57 is a leading candidate among the PDI family members, which could participate in ECM synthesis and stabilization, thus potentially characterizing a progressive renal fibrosis. We demonstrated that secreted ERP57 interacts with ECM proteins, such as fibronectin and collagen, and is supposed to prevent disulfide bond reduction and misfolding of these proteins, thus supporting regular extracellular accumulation. Bacitracin is poorly transported into mammalian cells, and even at high concentrations, it has minimal effects on the proliferative capacity of the cell. The combined treatment of the cells with TGFβ1 and bacitracin (for the inhibition of ERP57 secretion) substantially impaired ECM synthesis and extracellular accumulation. Moreover, inhibition of secretory ERP57 using specific monoclonal anti-ERP57 antibody resulted in a lower level of ECM proteins. The excretion of ERP57 in the urine of patients in earlier stages of renal fibrosis reveals the potential role of the secreted form as an earlier urinary marker for renal fibrosis before the onset of visible kidney damage. Furthermore, the amount of ERP57 excreted in urine was found to correlate with the level of tissue damage in an animal model for progressive renal fibrosis.

We demonstrated that rapid growing fibroblasts upon cytokine stimulation induce ER stress followed by protective UPR and increased expression of folding chaperones. This strongly supports the notion that the modulation of ER-stress proteins results in a reduction of ECM production and could have a substantially decreased fibrogenesis. Compounds that selectively inhibit UPR or stimulate ERAD activity could also be envisioned for renal fibrosis in which UPR seems to be pathologically activated. The ability of ERP57 inhibitors to impact disulfide oxidation and to abolish ECM accumulation strongly supports the potential of ERP57 as a therapeutic target in renal fibrosis.

Materials and Methods

DMEM (Dulbecco's modified Eagle's medium) was from Gibco. L-glutamine, urea and DTT were from Sigma. Culture flasks were from Falcon, CHAPS [(3-Cholamidopropyl)dimethylammonio]-1-propanesulfonate] was from MERCK. Precision plus protein marker and Bio-Lyte® were from Bio-Rad. BSA was from Roche. Protease inhibitor Mix 100 was from GE Healthcare. Lambda2 UV/VIS spectrophotometer was from Perkin-Elmer. Sequazyme™ Peptide Mass Standards Kit was from Applied Biosystems. Colloidal Coomasie blue staining (Roti-Blue) was from Carl-Roth. Monoclonal mouse anti-vimentin-antibody was from DAKO. Mouse anti-ERP57 monoclonal antibody and rabbit anti-ERP72 polyclonal antibody were from Stressgen. Mouse anti-β-actin monoclonal antibody and rabbit anti-GRP78/BiP polyclonal antibody were from Sigma. Mouse anti-CALR monoclonal antibody was from BD Bioscience. Rabbit anti-ERP57, anti-EIF2A mouse monoclonal, anti-pEIF2A mouse monoclonal and anti-CHOP mouse monoclonal antibodies were from Abcam. Bacitracin, T3 and AGT were from Sigma. TGFβ-1 and PDGF were from R&D Systems.

Animals

Col4a3-deficient and wild-type littermate mice in identical SvJ129 genetic backgrounds were selected from the available Alport disease models (Jackson Immunoresearch Laboratories, Westgrove, PA, USA) because of their consistent phenotype leading to progressive renal fibrosis and to uraemic death at approximately 10 weeks old (Cosgrove et al., 1996). All mice were bred under specific pathogen-free housing conditions and were genotyped using the polymerase chain reaction as described previously (Ninichuk et al., 2005). All experimental procedures were performed according to the German animal care and ethics legislation (NIH standards), and were approved by the local government authorities.

Cell line and culture procedure

Human renal fibroblasts cell line (TK173) used in these experiments was derived from a normal human kidney. The cells were immortalized by transfection with the plasmid pSV3gpt from SV4O and have typical morphological and biochemical properties of renal interstitial fibroblasts (Müller et al., 1995). The TK173 cell line was routinely maintained as a monolayer culture in 75 cm^2 tissue culture flasks (Falcon) in Dulbecco's modified Eagle's medium (Gibco), supplemented with

10% fetal calf serum (FCS, Gibco), 1% L-glutamine (PAA) and 1% penicillin/streptomycin (PAA). The second cell line culture consists of a renal epithelial cell designated HK-2 (human kidney-2). HK-2 was derived from a normal adult human renal cortex (Ryan et al., 1994). Cultured cells were exposed to a recombinant retrovirus containing the HPV 16 E6/E7 genes. The HK-2 cell line was maintained as a monolayer culture in Quantum 286 medium for epithelial cells (PAA) with 1% Penicillin/Streptomycin (Gibco). Cells were passaged at 85–90% confluency. Before the start of each experiment, normal growing cells were harvested with trypsin, and cultured in 7 ml medium at a density of 5×10^4 cells per flask and allowed to attach and grow overnight at 37℃ in a humidified atmosphere with 5% CO_2.

FCS-free cell culture and cell treatment

To identify new mechanisms and pathways associated with renal fibrosis, TGFβ1-mediated transition of renal cells to myofibroblasts was used as model. For this reason, TK173 or HK-2 cells were grown to subconfluency (~70% confluency) 75-cm^2 culture flasks. Medium was removed, and after washing in phosphate-buffered saline (PBS) the cells were incubated for a further 24 h in 10 ml serum-free DMEM. Purified human TGFβ1, PDGF (7 ng/ml) (R&D Systems, Minneapolis, MN, USA), AGT (Sigma-Aldrich, St Louis, MO, USA) or tunicamycin (5 µM) were added to the medium, and the transformation of fibroblasts to myofibroblasts was monitored at different times (24, 48, 72, 96 h and 2 weeks) in 10 ml serum-free DMEM. In parallel, supernatants and cell extracts were collected, and the proteins were processed as described below for further analyses.

To investigate the effect of BMP7 on TGFβ1-induced impairment of protein expression, renal cells were subjected for 48 h to treatment with TGFβ1. Subsequently a portion of the cells was treated with BMP7 (5 ng/ml) for an additional 48 h. The protein expression changes were examined using western blot analysis.

To investigate the proteome of the secreted proteins, TK173 and HK-2 cells were cultured in FCS free medium for 24 h. Subsequently the cells were treated with TGFβ1, PDGF or AGT for 24 h. The medium with the cytokines was changed to avoid any impact of dead cells on supernatant proteome, and the cells were incubated for additional 48 h with the three cytokines separately. The supernatant was collected and processed as described below.

Protein extraction and precipitation

The protein extraction was performed as described previously (Dihazi et al., 2011). To reduce the salt contamination and to enrich the proteins, chloroform-methanol precipitation was performed according to Wessel and Flügge (Wessel and Flügge, 1984).

For enrichment of the proteins before precipitation in supernatant samples, an ultrafiltration step using Vivacell 100 centrifugal filter device (5 kDa molecular weight cut-off; Sartorius, Goettingen, Germany) was performed. Centrifugation was carried out at 3000 ***g*** to reduce the volume of the supernatant to 500 µl. The resulting samples were subjected to chloroform-methanol precipitation as described above. For the western blot analysis of ECM proteins, the reducing agents (e.g. DTT) were avoided in lysis buffer to keep disulfide bridges intact.

Total protein concentration was estimated using the Bio-Rad protein assay (Bio-Rad, Hercules, CA, USA) according to Bradford (Bradford, 1976). BSA (Sigma, Steinheim, Germany) was used as a standard.

2-D gel electrophoresis

Large scale 2-DE and gel staining were carried out as described previously (Dihazi et al., 2011). For protein identification, 2-DE gels were additionally stained with collodial Coomassie blue, Roti-Blue (Roth, Karlsruhe, Germany) overnight.

2D-DIGE

Protein extraction and chloroform-methanol precipitation were performed as described above. The resulting pellet was solubilized in labelling buffer (30 mM Tris/HCl pH 8.5, 9.5 M urea, 2% CHAPS, 10 mM PMSF), centrifuged (5 min, 13,000 ***g***), and the protein concentration of the supernatant was determined as described above. The protein labelling with CyDyes and the 2-DE were performed as described previously (Dihazi et al., 2011). Fluorescent images were captured in 16-bit TIFF files format. Spot matching across gels and normalization based on the internal standard was performed using Delta2D software (Decodon, Greifswald, Germany). To analyze the significance of protein regulation, a Student's *t*-test was performed, and statistical significance was assumed for $P<0.01$. For protein identification, 2-DE gels were post-stained with colloidal Coomassie blue (Roti-Blue) overnight. Differentially regulated proteins were excised and processed for identification by MS.

Protein identification from 2-DE gels

In-gel digestion and peptide extraction were carried out as described previously (Dihazi et al., 2011). Subsequently the extracted peptides were subjected to peptide sequence analysis. The samples were dissolved in 0.1% formic acid and processed as described previously (Dihazi et al., 2011). Processed data were searched against MSDB and Swissprot databases through the Mascot search engine using a peptide mass tolerance of 50 ppm (parts per million) and fragment tolerance of 100 mmu (millimass unit). Protein identifications with at least two peptides sequenced were considered significant.

Indirect immunofluorescence staining

For the indirect immunofluorescence staining 30,000 cells were cultivated overnight in eight-well chamber slides. The medium was removed and the cells were washed twice with PBS-buffer. Fixation of the cells was carried out for 15 min at room temperature with 4% paraformaldehyde in PBS. After permeabilization with 0.1% Triton X-100 in PBS for 1 h, the fixed cells were blocked with 1% BSA (Sigma-Aldrich, St Louis, MO, USA) and PBS-buffer for 30 min and incubated overnight separately with the appropriate primary antibody. Alexa Fluor 488-conjugated goat anti-mouse antibodies or donkey anti-rabbit antibodies were used as secondary antibodies. They were incubated for 60 min at room temperature in the dark. The unbounded secondary antibody was removed with three successive wash steps with PBS-buffer for 10 min each. Thereafter, the samples were counterstained with DAPI in PBS-buffer for 5 min. Afterwards, samples were analyzed on an immunofluorescence Zeiss Axiophot microscope (Carl Zeiss, Jena, Germany) using the AnalySIS software (Soft Imaging Systems, Leinfelden, Germany).

Western blot analysis

Western blot analysis was performed according to Towbin and colleagues (Towbin et al., 1989; Towbin et al., 1992). 50 µg of the cell extracts were loaded per lane on a 12% SDS-gel after denaturation with Laemmli buffer (in the case of ECM proteins without reducing agents). Antibodies against rabbit ERP57, rabbit GRP78, rabbit CALR, mouse EIF2A, phosphorylated EIF2A, mouse CHOP, rabbit IRE1A, rabbit phosphorylated EREA, rabbit PERK, rabbit phosphorylated PERK, rabbit ATF6A and mouse cleved ATF6, used as the primary antibodies, were diluted in blocking buffer, then added to the membrane and allowed to incubate for 60 min. Molecular Probes® Alexa Fluor 647 goat anti-mouse IgG antibody or Alexa Fluor 647 goat anti-rabbit IgG antibody, and Alexa Fluor 680 goat anti-mouse IgG antibody or Alexa Fluor 680 goat anti-rabbit antibody were used as secondary antibodies. Before imaging, the blots were dried in the dark. The blot membranes were scanned at a resolution of 50 µm on a Fuji FLA-5100 scanner (Fuji Photo, Kanagawa, Japan) with single laser-emitting excitation light at 635 nm and 670 nm, respectively.

In the case of *Col4a3* knockout mice, three animals per group were killed at weeks 4, 6, 7 and 9, and as a control three wild-type animals were used. The kidneys from all animals were harvested. Aliquots of tissue extracts from three kidneys of different animals (40 µg protein) were dissolved in SDS-sample buffer, separated by electrophoresis in a SDS-polyacrylamide gel (12.5%) under reducing conditions, transferred to a nitrocellulose membrane, and blocked for 60 min at room temperature with 5% milk-powder in a 0.2 mol/L Tris-HCl buffer, pH 7.6, containing 0.1% Tween 20 solution (TBST buffer). Antibodies against rabbit ERP57, rabbit GRP78, and rabbit CALR as the primary antibodies were diluted in blocking buffer, then added to the membrane and allowed to incubate for 60 min. The addition of secondary antibodies, membrane scanning and analysis were performed as described above.

Urine collection and analysis of ERP57 excretion

The collection of urine samples and analysis were approved by the local Institutional Ethics Review Committee of the University Medical Centre, Georg-August University, Goettingen (Germany). All patients had given their informed consent before the study. Urine samples (20 ml) were collected from 15 diabetic patients with lower microalbuminuria (20–50 mg/l), 15 patients with AKI and 15 healthy individuals. The collection and preparation of urine samples was performed according to the EuroKup/HKUPP urine protocol and recommendation (http://www.eurokup.org/). Second morning midstream urine was used. Urine samples were collected from the examinees, centrifuged at 1000 ***g*** for 10 min at 4℃ to remove cell debris and casts. The supernatant was aliquoted (1 mL aliquots) without disturbing the pellets and was stored at −80℃ until use.

In case of animal model of fibrosis, urine was sampled by placing mice in metabolic cages. Samples from five different wild-type mice and from five mice from each group from 4, 6, 7 and 9 weeks *Col4a3* knockout mice were collected. 30 µl of urine were used for western blot analysis. Protein precipitation and western blot analysis were performed as described above.

Protein immunoprecipitation

For protein–protein interaction studies, immunoprecipitation (IP) using protein G-Agarose matrix was performed. The cell secretome was harvested from treated cells as described above and concentrated to 500 µl. 200 µg secretome proteins were used for immunoprecipitation. The samples were adjusted to 1 ml with PBS buffer and 5 µl monoclonal anti-*ERP57* or monoclonal anti-FIN antibodies were added. The samples were incubated overnight at 4℃ under agitation. 70 µl protein

G-Agarose matrix (Roche) was added to each sample. The mixture was incubated at 4℃ under rotary agitation for 4 h. The samples were centrifuged and the supernatant removed. The agarose matrix was washed three times with PBS buffer. The supernatant was removed and 30 µl of 2×loading buffer were added, the samples were boiled at 95℃ for 5 min to denature the proteins and separate them from the protein G-Agarose, and then centrifuged. The supernatant was used to run SDS-PAGE and identify the bind proteins.

MTT cell viability assay

For the cell proliferation assay the cell proliferation Kit I (MTT) from Roche was used according to the manufacturer's instructions. To investigate the effect of PDI inhibitors bacitracin and tri-iodothyronine (T3) on cell viability and proliferation, 8000–10,000 cells were grown in a 96-well tissue culture plate in FCS-free medium as a control, or supplemented with either bacitracin (100–500 µM) or T3 (50–200 µM). All analyses were performed in triplicate.

PDI activity in insulin turbimetric assay

The PDI activity assay was performed by measuring insulin disulfide reduction according to Lundström and Holmgren (Lundström and Holmgren, 1990). The effect of the inhibitors on PDI activity was tested by adding bacitracin (250 µM), triiodothyronine (T3) (100 µM), and antibodies against ERP72 or ERP57 (10 µg/ml) to the reagent mixture 10 min before starting the reaction. The change in activity was monitored by measuring the insulin precipitation.

Effect of protein disulfide isomerase inhibition on ECM synthesis

To test the effect of PDI inhibitors on ECM synthesis and accumulation, TK173 were cultured in FCS-free medium as described above. PDI inhibitors (bacitracin, T3, and antibodies against ERP57 or ERP72) were added at the concentration with the maximum effect 4 h before treatment with TGFβ1. Subsequently, the cells were incubated for 72 h. The impact of the inhibition on TK173 transformation and on ECM synthesis was monitored using western blot analysis.

siRNA construct and transfection

siRNA oligonucleotides specific for the knockdown of ERP57 expression (sense strand: 5′-ACCTCGTCCTTCACATCTCACTAACATCAAGAGTGTTAGTG-AGATGTGAAGGACTT-3′), (antisense strand: 3′-CAAAAAGTCCTTC-ACATCTCACTAACACTCTTGATGTTAGTGAGATGTGAAGGACG-5′) were designed in our laboratory and synthesized by Eurofins MWG Operon (Germany). siRNA vector was constructed by ligating oligonucleotides in psiRNAh7SK neo vector (Invitrogen). All constructs were verified by sequencing. TK173 cells cultured to ~80% confluency were transfected with the vector containing siRNA for the ERP57 knockdown using transfection reagent Lipofectamine 2000™ (Invitrogen) according to the standard protocol of the manufacturer. Cells transfected with psiRNAh7SK without siRNA for ERP57 were used as a positive control. The transfection medium was removed after 24 h and replaced with normal culture media supplemented with 0.5 mg/ml G-418 (Invitrogen) as a selection factor for stable transfection. Cells were maintained in the selective medium for 14 days to achieve stable transfection. The expression of ERP57 was assessed by western blot analysis and immunofluorescence staining. The impact of ERP57 knockdown on ECM protein folding and accumulation was monitored by western blot analysis and immunofluorescence staining. For comparison, the cells were treated with the reducing agent dithiothreitol (1 mM) for 30 min before staining.

Statistical analysis

For 2-DE the digitalized images were analyzed; spot matching across gels and normalization were performed using Delta2D 3.4 (Decodon, Braunschweig, Germany). Delta2D computes a 'spot quality' value for every spot detected. This value shows how closely a spot represents the 'ideal' 3D Gaussian bell shape. On the basis of the average spot volume ratio, spots whose relative expression is changed at least twofold (increase or decrease) between the compared samples were considered to be significant. To analyze the significance of protein regulation, Student's *t*-test was performed, and statistical significance was assumed for $P<0.01$.

All blots were quantified using the ImageJ software. For comparison between two measures (in the same group) the paired *t*-test was used. The unpaired *t*-test (for comparing two groups) or one-way ANOVA (comparing three or more groups) were used. The data were compiled using the software package GraphPad Prism, version 4. The software was used for graphical presentation. Results are presented as the mean ± s.d. of at least three independent experiments. Differences were considered statistically significant when $P<0.05$.

Acknowledgements

We thank Elke Brunst-Knoblich for technical assistance.

Author contributions

H.D. designed the study performed the majority of experiments and wrote the article, and revised the article critically; G.H.D. performed the proteomics analysis, wrote the article and helped with data interpretation; A.B. and M.E. performed the experiments involving the animal model; C.A.M. provided the cell lines and was also involved in revising the manuscript; A.R.A. was responsible for the acquisition of the mass spectrometry data; D.R. was involved in animal model experiments and urine collection; R.V. assisted in the experiments involving cytokine treatments; G.A.M. helped in the study design and manuscript writing, and revised the article critically.

Funding

This research received no specific grant from any funding agency in the public, commercial or not-for-profit sectors.

Supplementary material available online at
http://jcs.biologists.org/lookup/suppl/doi:10.1242/jcs.125088/-/DC1

References

Ahamed, J., Versteeg, H. H., Kerver, M., Chen, V. M., Mueller, B. M., Hogg, P. J. and Ruf, W. (2006). Disulfide isomerization switches tissue factor from coagulation to cell signaling. *Proc. Natl. Acad. Sci. USA* **103**, 13932-13937.

Akagi, S., Yamamoto, A., Yoshimori, T., Masaki, R., Ogawa, R. and Tashiro, Y. (1988). Localization of protein disulfide isomerase on plasma membranes of rat exocrine pancreatic cells. *J. Histochem. Cytochem.* **36**, 1069-1074.

Bechtel, W., McGoohan, S., Zeisberg, E. M., Müller, G. A., Kalbacher, H., Salant, D. J., Müller, C. A., Kalluri, R. and Zeisberg, M. (2010). Methylation determines fibroblast activation and fibrogenesis in the kidney. *Nat. Med.* **16**, 544-550.

Bedard, K., Szabo, E., Michalak, M. and Opas, M. (2005). Cellular functions of endoplasmic reticulum chaperones calreticulin, calnexin, and ERp57. *Int. Rev. Cytol.* **245**, 91-121.

Bradford, M. M. (1976). A rapid and sensitive method for the quantitation of microgram quantities of protein utilizing the principle of protein-dye binding. *Anal. Biochem.* **72**, 248-254.

Branton, M. H. and Kopp, J. B. (1999). TGF-beta and fibrosis. *Microbes Infect.* **1**, 1349-1365.

Cosgrove, D., Meehan, D. T., Grunkemeyer, J. A., Kornak, J. M., Sayers, R., Hunter, W. J. and Samuelson, G. C. (1996). Collagen COL4A3 knockout: a mouse model for autosomal Alport syndrome. *Genes Dev.* **10**, 2981-2992.

Dihazi, H., Dihazi, G. H., Jahn, O., Meyer, S., Nolte, J., Asif, A. R., Mueller, G. A. and Engel, W. (2011). Multipotent adult germline stem cells and embryonic stem cells functional proteomics revealed an important role of eukaryotic initiation factor 5A (Eif5a) in stem cell differentiation. *J. Proteome Res.* **10**, 1962-1973.

Djamali, A. (2007). Oxidative stress as a common pathway to chronic tubulointerstitial injury in kidney allografts. *Am. J. Physiol.* **293**, F445-F455.

Dobson, C. M. (2003). Protein folding and misfolding. *Nature* **426**, 884-890.

Eitner, F. and Floege, J. (2005). Therapeutic targets for prevention and regression of progressive fibrosing renal diseases. *Curr. Opin. Investig. Drugs* **6**, 255-261.

Ellerman, D. A., Myles, D. G. and Primakoff, P. (2006). A role for sperm surface protein disulfide isomerase activity in gamete fusion: evidence for the participation of ERp57. *Dev. Cell* **10**, 831-837.

Ellgaard, L. and Frickel, E. M. (2003). Calnexin, calreticulin, and ERp57: teammates in glycoprotein folding. *Cell Biochem. Biophys.* **39**, 223-247.

Fenouillet, E., Barbouche, R., Courageot, J. and Miquelis, R. (2001). The catalytic activity of protein disulfide isomerase is involved in human immunodeficiency virus envelope-mediated membrane fusion after CD4 cell binding. *J. Infect. Dis.* **183**, 744-752.

Frand, A. R., Cuozzo, J. W. and Kaiser, C. A. (2000). Pathways for protein disulphide bond formation. *Trends Cell Biol.* **10**, 203-210.

Freedman, R. B. (1989). Protein disulfide isomerase: multiple roles in the modification of nascent secretory proteins. *Cell* **57**, 1069-1072.

Goldberg, A. L. (2003). Protein degradation and protection against misfolded or damaged proteins. *Nature* **426**, 895-899.

Harris, R. C. and Neilson, E. G. (2006). Toward a unified theory of renal progression. *Annu. Rev. Med.* **57**, 365-380.

Hebert, D. N. and Molinari, M. (2007). In and out of the ER: protein folding, quality control, degradation, and related human diseases. *Physiol. Rev.* **87**, 1377-1408.

Hirschberg, R. (2005). Wound healing in the kidney: complex interactions in renal interstitial fibrogenesis. *J. Am. Soc. Nephrol.* **16**, 9-11.

Iwano, M. and Neilson, E. G. (2004). Mechanisms of tubulointerstitial fibrosis. *Curr. Opin. Nephrol. Hypertens.* **13**, 279-284.

Jessop, C. E., Chakravarthi, S., Garbi, N., Hämmerling, G. J., Lovell, S. and Bulleid, N. J. (2007). ERp57 is essential for efficient folding of glycoproteins sharing common structural domains. *EMBO J.* **26**, 28-40.

Kim, I., Xu, W. and Reed, J. C. (2008). Cell death and endoplasmic reticulum stress: disease relevance and therapeutic opportunities. *Nat. Rev. Drug Discov.* **7**, 1013-1030.

Lahav, J., Jurk, K., Hess, O., Barnes, M. J., Farndale, R. W., Luboshitz, J. and Kehrel, B. E. (2002). Sustained integrin ligation involves extracellular free sulfhydryls and enzymatically catalyzed disulfide exchange. *Blood* **100**, 2472-2478.

Lahav, J., Wijnen, E. M., Hess, O., Hamaia, S. W., Griffiths, D., Makris, M., Knight, C. G., Essex, D. W. and Farndale, R. W. (2003). Enzymatically catalyzed disulfide exchange is required for platelet adhesion to collagen via integrin alpha2beta1. *Blood* **102**, 2085-2092.

Lassila, M., Fukami, K., Jandeleit-Dahm, K., Semple, T., Carmeliet, P., Cooper, M. E. and Kitching, A. R. (2007). Plasminogen activator inhibitor-1 production is pathogenetic in experimental murine diabetic renal disease. *Diabetologia* **50**, 1315-1326.

Lee, E. A., Seo, J. Y., Jiang, Z., Yu, M. R., Kwon, M. K., Ha, H. and Lee, H. B. (2005). Reactive oxygen species mediate high glucose-induced plasminogen activator inhibitor-1 up-regulation in mesangial cells and in diabetic kidney. *Kidney Int.* **67**, 1762-1771.

Lewis, M. J., Sweet, D. J. and Pelham, H. R. (1990). The ERD2 gene determines the specificity of the luminal ER protein retention system. *Cell* **61**, 1359-1363.

Liu, Y. (2006). Renal fibrosis: new insights into the pathogenesis and therapeutics. *Kidney Int.* **69**, 213-217.

Lundström, J. and Holmgren, A. (1990). Protein disulfide-isomerase is a substrate for thioredoxin reductase and has thioredoxin-like activity. *J. Biol. Chem.* **265**, 9114-9120.

Markovic, I., Stantchev, T. S., Fields, K. H., Tiffany, L. J., Tomiç, M., Weiss, C. D., Broder, C. C., Strebel, K. and Clouse, K. A. (2004). Thiol/disulfide exchange is a prerequisite for CXCR4-tropic HIV-1 envelope-mediated T-cell fusion during viral entry. *Blood* **103**, 1586-1594.

Müller, G. A., Frank, J., Rodemann, H. P. and Engler-Blum, G. (1995). Human renal fibroblast cell lines (tFKIF and tNKF) are new tools to investigate pathophysiologic mechanisms of renal interstitial fibrosis. *Exp. Nephrol.* **3**, 127-133.

Nangaku, M. (2006). Chronic hypoxia and tubulointerstitial injury: a final common pathway to end-stage renal failure. *J. Am. Soc. Nephrol.* **17**, 17-25.

Ninichuk, V., Gross, O., Reichel, C., Khandoga, A., Pawar, R. D., Ciubar, R., Segerer, S., Belemezova, E., Radomska, E., Luckow, B. et al. (2005). Delayed chemokine receptor 1 blockade prolongs survival in collagen 4A3-deficient mice with Alport disease. *J. Am. Soc. Nephrol.* **16**, 977-985.

Oyadomari, S. and Mori, M. (2004). Roles of CHOP/GADD153 in endoplasmic reticulum stress. *Cell Death Differ.* **11**, 381-389.

Primm, T. P. and Gilbert, H. F. (2001). Hormone binding by protein disulfide isomerase, a high capacity hormone reservoir of the endoplasmic reticulum. *J. Biol. Chem.* **276**, 281-286.

Qi, W., Chen, X., Poronnik, P. and Pollock, C. A. (2006). The renal cortical fibroblast in renal tubulointerstitial fibrosis. *Int. J. Biochem. Cell Biol.* **38**, 1-5.

Rao, R. V. and Bredesen, D. E. (2004). Misfolded proteins, endoplasmic reticulum stress and neurodegeneration. *Curr. Opin. Cell Biol.* **16**, 653-662.

Raykhel, I., Alanen, H., Salo, K., Jurvansuu, J., Nguyen, V. D., Latva-Ranta, M. and Ruddock, L. (2007). A molecular specificity code for the three mammalian KDEL receptors. *J. Cell Biol.* **179**, 1193-1204.

Reinhardt, C., von Brühl, M. L., Manukyan, D., Grahl, L., Lorenz, M., Altmann, B., Dlugai, S., Hess, S., Konrad, I., Orschiedt, L. et al. (2008). Protein disulfide isomerase acts as an injury response signal that enhances fibrin generation via tissue factor activation. *J. Clin. Invest.* **118**, 1110-1122.

Ryan, M. J., Johnson, G., Kirk, J., Fuerstenberg, S. M., Zager, R. A. and Torok-Storb, B. (1994). HK-2: an immortalized proximal tubule epithelial cell line from normal adult human kidney. *Kidney Int.* **45**, 48-57.

Ryser, H. J., Levy, E. M., Mandel, R. and DiSciullo, G. J. (1994). Inhibition of human immunodeficiency virus infection by agents that interfere with thiol-disulfide interchange upon virus-receptor interaction. *Proc. Natl. Acad. Sci. USA* **91**, 4559-4563.

Schott, P., Singer, S. S., Kögler, H., Neddermeier, D., Leineweber, K., Brodde, O. E., Regitz-Zagrosek, V., Schmidt, B., Dihazi, H. and Hasenfuss, G. (2005). Pressure overload and neurohumoral activation differentially affect the myocardial proteome. *Proteomics* **5**, 1372-1381.

Schröder, M. and Kaufman, R. J. (2005). ER stress and the unfolded protein response. *Mutat. Res.* **569**, 29-63.

Szegezdi, E., Logue, S. E., Gorman, A. M. and Samali, A. (2006). Mediators of endoplasmic reticulum stress-induced apoptosis. *EMBO Rep.* **7**, 880-885.

Towbin, H., Staehelin, T. and Gordon, J. (1989). Immunoblotting in the clinical laboratory. *J. Clin. Chem. Clin. Biochem.* **27**, 495-501.

Towbin, H., Staehelin, T. and Gordon, J. (1992). Electrophoretic transfer of proteins from polyacrylamide gels to nitrocellulose sheets: procedure and some applications. 1979. *Biotechnology* **24**, 145-149.

Wessel, D. and Flügge, U. I. (1984). A method for the quantitative recovery of protein in dilute solution in the presence of detergents and lipids. *Anal. Biochem.* **138**, 141-143.

Zeisberg, M., Shah, A. A. and Kalluri, R. (2005). Bone morphogenic protein-7 induces mesenchymal to epithelial transition in adult renal fibroblasts and facilitates regeneration of injured kidney. *J. Biol. Chem.* **280**, 8094-8100.

Journal of Cell Science

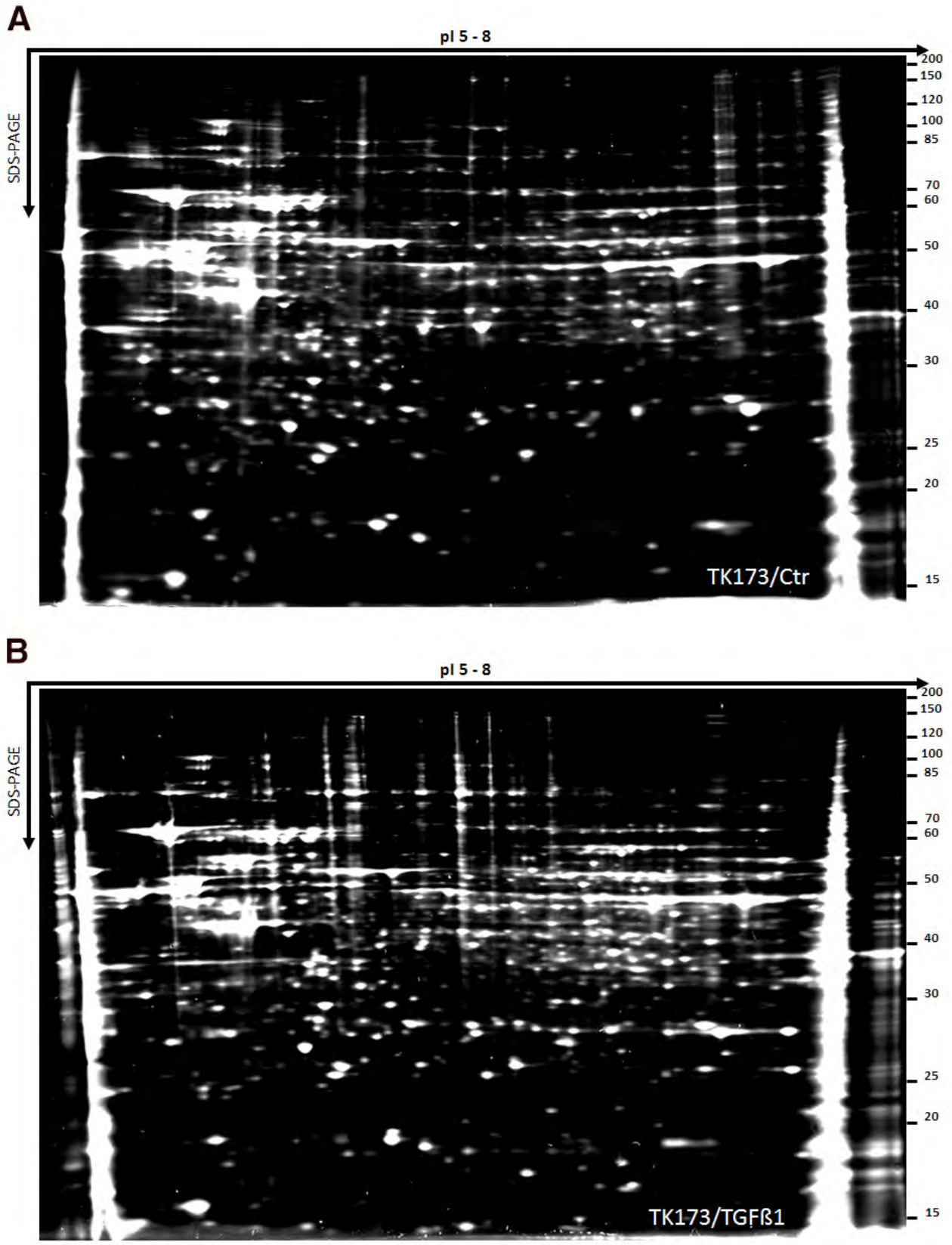

Fig. S1. 2-DE protein map of total protein isolated from control and TGFβ1 treated TK173 cells. 150 µg proteins were loaded on a 11-cm IPG strip with a linear pH 5–8 gradient for isoelectric focusing, and a 12% SDS-polyacrylamide gel was used for SDS-PAGE. Proteins were stained with flamingo A: TK173 control B: TK173/TGFβ1.

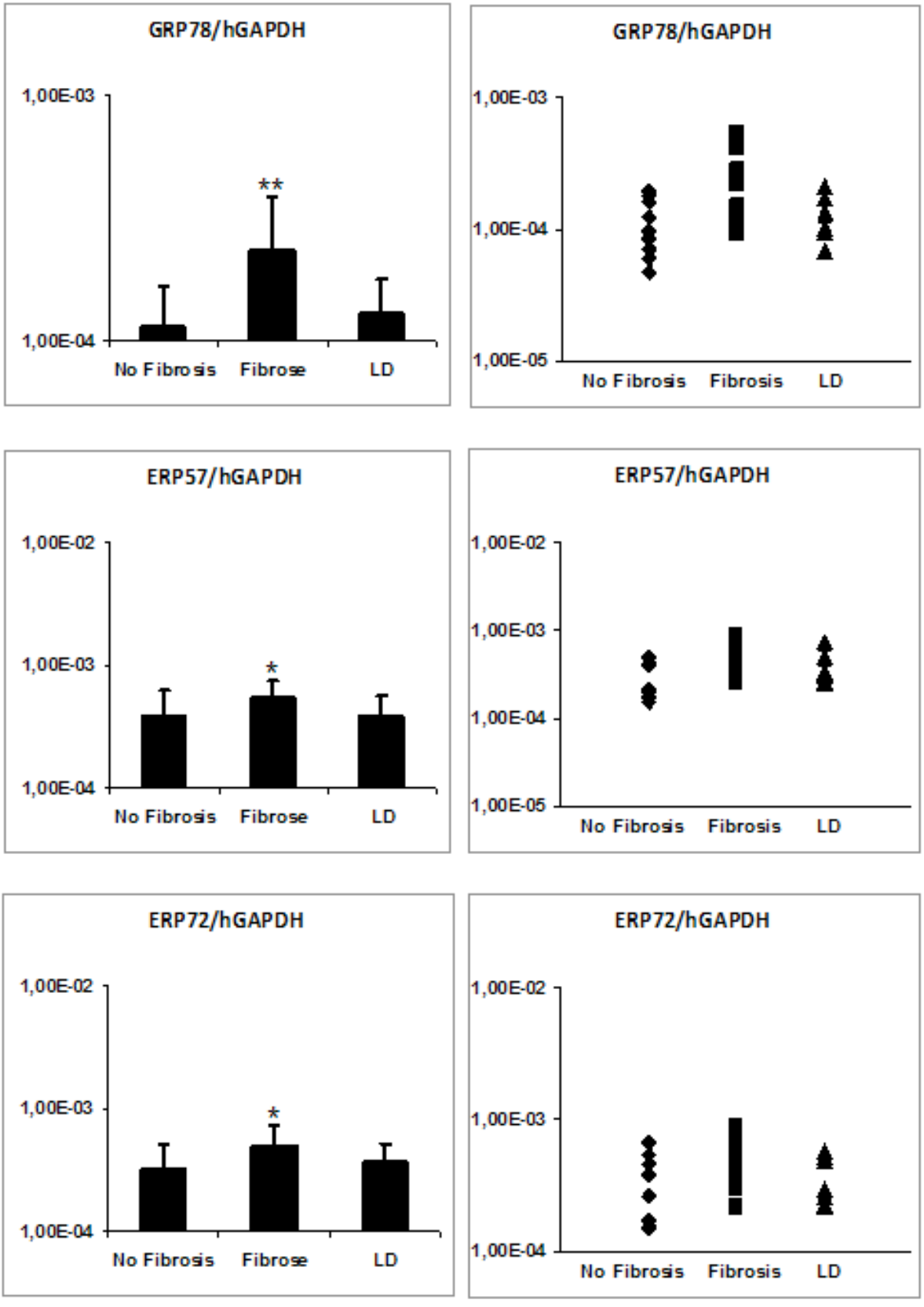

Fig. S2. Tubulointerstitial expression of ERP57, ERP72, GRP78 mRNA in biopsy material from patients with fibrotic kidneys (fibrosis) (n=15) examined with quantitative real-time reverse transcription PCR after tissue microdissection. Cadaveric kidneys (LD) (n=10) and non-fibrotic primary or secondary nephropathies (No Fibrosis) (n=10) served as controls. Results are expressed as ERP57, ERP72, or GRP78/GAPDH ratio. Mean values ± s.d. are shown. *P<0.045 **P<0.001 compared with control or to no fibrosis.

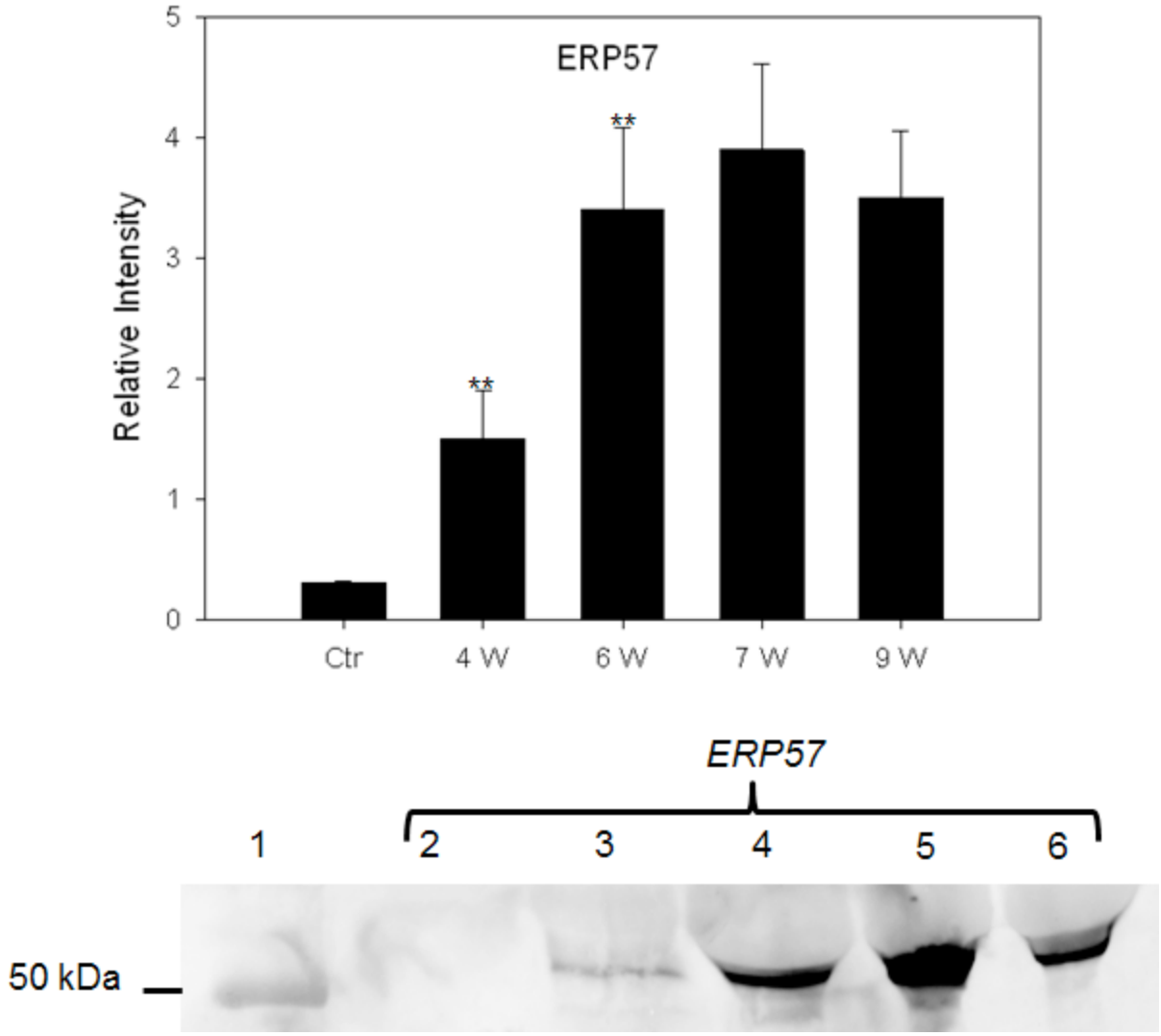

Fig. S3. Urine was sampled by placing mice in metabolic cages. Samples from 5 different wild type mice and from 5 mice from each group 4 (2), 6 (3), 7 (4), and 9 (5) weeks Col4a3 knockout mice were collected. Thirty micro liters of urine per animal were used for Western blot analysis. ERP57 excretion levels in mice urine were quantified using Western blot. On the y-axis the line-volume-percentage is given and the x-axis shows distribution of the intensity thought the corresponding urine group where the protein was analysed. The detection of proteins within experimental groups on blotting membrane was presented under the graph. Statistical analysis were performed by Prizma4 software (***P<0.001). 1: Molecular weight marker.

Supplemental Table 1: List of proteins identified from TGFß1 treated and non-treated TK173. The accession number in Swiss-Prot, the PMF and MS/MS information are given. The spots where MS/MS-data are missing were only identified with PMF.

Nr.	Protein name	Gene name	Swiss Prot Acc. Nr.	Nominal Mass	PMF	MS/MS score
1	Low molecular weight phosphotyrosine protein phosphatase	ACP1	P24666	18031		103
2	Actin, aortic smooth muscle	ACTA2	P62736	42009		152
3	Actin, cytoplasmic 1	ACTB	P60709	41710		117
4	Actin, cytoplasmic 1	ACTB	P60709	41710		349
5	Actin, cytoplasmic 1	ACTB	P60709	41710	79	106
6	Actin, cytoplasmic 2	ACTG1	P63261	41766	73	145
7	Actin, cytoplasmic 2	ACTG1	P63261	41766	93	89
8	Actin, cytoplasmic 2	ACTG1	P63261	41766	125	175
9	Actin, cytoplasmic 2	ACTG1	P63261	41766		214
10	Actin, cytoplasmic 2	ACTG1	P63261	41766	67	
11	Alpha-actinin-1	ACTN1	P12814	102993	109	
12	Alpha-actinin-1	ACTN1	P12814	102993		63
13	Alpha-actinin-1	ACTN1	P12814	102993		70
14	Alpha-actinin-1	ACTN1	P12814	102993		110
15	Alpha-actinin-1	ACTN1	P12814	102993		92
16	BAG family molecular chaperone regulator 2	BAG2	Q95816	23757		60
17	UPF0568 protein C14orf166	C14orf166	Q9Y224	28068	81	
18	Caldesmon	CALD1	Q05682	93194		173
19	Calreticulin	CALR	P27797	48142		210
20	Caprin-1	CAPRIN1	Q14444	78318		122
21	Chloride intracellular channel protein 1	CLIC1	O00299	26906	112	
22	Chloride intracellular channel protein 1	CLIC1	O00299	26906		98
23	Calponin-2	CNN2	Q99439	33675		70
24	CNN2 protein	CNN2	Q6FHE4	33709	151	
25	Collagen alpha-1(I) chain	COL1A1	P02452	138941		93
26	Collagen alpha-1(I) chain	COL1A1	P02452	138941		185
27	Collagen alpha-1(I) chain	COL1A1	P02452	138941		251
28	Collagen alpha-1(I) chain	COL1A1	P02452	138941		150
29	Collagen alpha-1(I) chain	COL1A1	P02452	138941		213
30	Cystatin-B	CSTB	P04080	11133		92
31	Desmin	DES	P17661	53536		132
32	Eukaryotic translation initiation factor 1	EIF1	P41567	12725		78
33	Endoplasmic reticulum resident protein 29	ERP29	P30040	28993		95
34	Protein disulfide-isomerase	ERP57	P30101	56747	101	
35	Protein disulfide-isomerase	ERP57	P30101	56747		151
36	Protein disulfide-isomerase	ERP57	P30101	56747		213
37	Protein disulfide-isomerase A4	ERP72	P13667	72932		165
38	Fatty acid-binding protein, epidermal	FABP5	Q01469	15164		78
39	Fibronectin	FN1	P02751	262442		115
40	Fibronectin	FN1	P02751	262442		157
41	Fibronectin	FN1	P02751	262442		97
42	Fibronectin	FN1	P02751	262442		81
43	Fibronectin	FN1	P02751	262442		68
44	Fibronectin	FN1	P02751	262442		121
45	Fibronectin	FN1	P02751	262442		89
46	Fibronectin	FN1	P02751	262442		145
47	Fibronectin	FN1	P02751	262442		132
48	78 kDa glucose-regulated protein	GRP78	P11021	72288	61	151
49	78 kDa glucose-regulated protein	GRP78	P11021	72288	257	
50	Endoplasmin	GRP94	P14625	92411		87
51	Endoplasmin	GRP94	P14625	92411	145	151
52	Endoplasmin	GRP94	P14625	92411	108	
53	Endoplasmin	GRP94	P14625	92411		122
54	Endoplasmin	GRP94	P14625	92411		157
55	Endoplasmin	GRP94	P14625	92411		231

56	Endoplasmin	GRP94	P14625	92411	165	
57	Endoplasmin	GRP94	P14625	92411	110	
58	Endoplasmin	GRP94	P14625	92411	125	
59	Glutathione S-transferase P	GSTP1	P09211	23341		187
60	Histidine triad nucleotide-binding protein 1	HINT1	P49773	13793		45
61	Histone H2B type 1-B	HIST1H2BB	P33778	13942		209
62	Heterogeneous nuclear ribonucleoprotein A/B	HNRNPAB	Q99729	36225		125
63	Heterogeneous nuclear ribonucleoprotein H	HNRNPH1	P31943	49229		105
64	Heterogeneous nuclear ribonucleoprotein H3	HNRNPH3	P31942	36926		105
65	Heterogenous nuclear ribonuclear protein K	HNRNPK	P61978	50944		229
66	Heterogeneous nuclear ribonucleoprotein D-like	HNRPDL	O14979	46438	89	
67	78 kDa glucose-regulated protein	HSPA5	P11021	72288		395
68	78 kDa glucose-regulated protein	HSPA5	P11021	72288		157
69	78 kDa glucose-regulated protein	HSPA5	P11021	72288	74	
70	Hypoxia up-regulated protein 1	HYOU1	Q61N67	111266		416
71	Inosine-5'-monophosphate dehydrogenase 2	IMPDH2	P12268	55770		42
72	LIM and SH3 domain protein 1	LASP1	Q14847	29717		98
73	Galectin 1	LGALS1	P09382	14706		157
74	NADH dehydrogenase[ubiquinone] flavoprotein 2, mitochondrial	NDUFV2	P19404	27374		109
75	Protein DJ-1	PARK7	Q99497	19891		135
76	PEST proteolytic signal-containing nuclear protein	PCNP	Q8WW12	18913		72
77	PEST proteolytic signal-containing nuclear protein	PCNP	Q8WW12	18913		96
78	Protein disulfide-isomerase	PDI	P07237	57116		133
79	Pyruvate kinase isozymes M1/M2	PKM2	P14618	57937		145
80	Peptidyl-prolyl cis-trans isomerase A	PPIA	P62937	18001	100	
81	Peptidyl-prolyl cis-trans isomerase A	PPIA	P62937	18001		123
82	Peptidyl-prolyl cis-trans isomerase A	PPIA	P62937	18001		111
83	Peptidyl-prolyl cis-trans isomerase A	PPIA	P62937	18001	125	
84	Peroxiredoxin-1	PRDX1	Q06830	22110		96
85	Peroxiredoxin-2	PRDX2	P32119	21892		158
86	Thioredoxin-dependent peroxide reductase, mitochondrial	PRDX3	P30048	27675		218
87	Peroxiredoxin-6	PRDX6	P30041	25035		215
88	Proteasome subunit beta type-6	PSMB6	P28072	25341		119
89	GTP-binding nuclear protein Ran	RAN	P62826	24423		92
90	RNA-binding protein 8A	RBM8A	Q9Y5S9	19877		151
91	40S ribosomal protein S12	RPS12	P25398	14515	88	
92	Splicing factor, arginine/serine-rich 1	SFRS1	Q07955	27728	96	
93	Splicing factor, arginine/serine-rich 1	SFRS1	Q07955	27728	56	
94	Superoxide dismutase [Cu-Zn]	SOD1	P00441	15936		112
95	Superoxide dismutase [Mn], mitochondrial	SOD2	P04179	24722		154
96	Tubulin-specific chaperone A	TBCA	O75347	12847		89
97	Triosphosphate isomerase	TPI1	P60174	26653		127
98	Tubulin alpha-1A chain	TUBA1A	Q71036	50104	100	
99	Tubulin alpha-1A chain	TUBA1A	Q71036	50104		121
100	Tubulin alpha-1C chain	TUBA1C	Q9BQE3	49863	138	
101	Tubulin alpha-1C chain	TUBA1C	Q9BQE3	49863		85
102	Tubulin alpha-1C chain	TUBA1C	Q9BQE3	49863	70	
103	Tubulin alpha-1C chain	TUBA1C	Q9BQE3	49863	198	
104	Tubulin alpha-1C chain	TUBA1C	Q9BQE3	49863	151	
105	Tubulin alpha-1C chain	TUBA1C	Q9BQE3	49863	165	
106	Tubulin alpha-1C chain	TUBA1C	Q9BQE3	49863	145	
107	Thioredoxin	TXN	P10599	11730		168
108	Thioredoxin	TXN	P10599	11730	112	
109	Ubiquitin-conjugating enzyme E2 N	UBE2N	P61088	17127	141	
110	Vinculin	VCL	P18206	123799		98
111	Transitional endoplasmic reticulum ATPase	VCP	P55072	89266		210
112	Vimentin	VIM	P08670	53619		340
113	Vimentin	VIM	P08670	53619		125
114	Vimentin	VIM	P08670	53619		235

Supplemental Table 2: List of proteins identified from immunoprecipitation using anti-ERP57 antibody and G-protein agarose matrix. The gene name, accession number in Swiss-Prot, protein mass, and MS/MS information are given

Protein name	Gene name	Swiss Prot Acc. Nr.	Mass	MS/MS	Peptide sequenced
Histone H4	HIST1H4A	P62805	11360	492	17
Profilin-1	PFN1	P07737	15045	104	2
Histone H2B type 1-D	HIST1H2BD	P58876	13928	243	13
Peptidyl-prolyl cis-trans isomerase A	PPIA	P62937	18001	250	6
Cofilin-1	CFL1	P23528	18491	285	7
Peptidyl-prolyl cis-trans isomerase B	PPIB	P23284	23728	172	4
Ras-related protein Rab-7a	RAB7A	P51149	23475	367	7
Peroxiredoxin-1	PRDX1	Q06830	22096	224	6
Peroxiredoxin-1	PRDX1	Q06830	22096	478	22
Peroxiredoxin-1	PRDX1	Q06830	22096	250	7
GTP-binding nuclear protein Ran	RAN	P62826	24408	324	11
Heat shock protein beta-1	HSPB1	P04792	22768	543	32
Renin receptor	ATP6AP2	O75787	38983	365	11
Prohibitin	PHB	P35232	29786	624	12
Annexin A5	ANXA5	P08758	35914	645	21
Glyceraldehyde-3-phosphate dehydrogenase	GAPDH	P04406	36030	553	27
Actin, cytoplasmic 1	ACTB	P60709	41710	377	15
Actin, cytoplasmic 2	ACTG1	P63261	41766	727	44
Alpha-enolase	ENO1	P06733	47139	420	11
Protein disulfide isomerase family A, member 6	PDIA6	Q53RC7	48121	870	34
Protein disulfide isomerase A3	ERP57	P30101	56782	688	24
Protein disulfide isomerase A3	ERP57	P30101	56782	370	8
Transforming growth factor-beta-induced protein ig-h3	TGFBI	Q15582	74634	180	5
78 kDa glucose-regulated protein	HSPA5	P11021	72288	754	16
Heat shock protein HSP 90-beta	HSP90AB1	P08238	83212	651	18
Endoplasmin	HSP90B1	P14625	92411	730	25
Neutral alpha-glucosidase AB	GANAB	Q14697	106807	378	16
Integrin alpha-V	ITGAV	P06756	115964	195	6
Clathrin heavy chain 1	CLTC	Q00610	191493	418	13
Myosin-9	MYH9	P35579	226392	830	22
Fibronectin	FN1	P02751	262460	1143	25
Collagen alpha-1(I) chain	COL1A1	P02452	138,941	982	21

Supplemental Table 3
List of proteins identified from immunoprecipitation using anti-FIN antibody and G-protein agarose matrix. The gene name, accession number in Swiss-Prot, protein mass, and MS/MS information are given.

Protein name	Gene name	Swiss Prot Acc. Nr.	Mass	MS/MS	Number of sequenced Peptides
Fibronectin	FN1	P02751	262460	297	8
Fibronectin	FN1	P02751	262460	197	13
Fibronectin	FN1	P02751	262460	129	8
Fibronectin	FN1	P02751	262460	161	5
Fibronectin	FN1	P02751	262460	55	5
Fibronectin	FN1	P02751	262460	131	2
Fibronectin	FN1	P02751	262460	351	7
Fibronectin	FN1	P02751	262460	162	6
Endoplasmin	HSP90B1	P14625	92411	24	1
Endoplasmin	HSP90B1	P14625	92411	155	15
Myosin-9	MYH9	P35579	226392	45	9
Myosin-9	MYH9	P35579	226392	204	8
Myosin-9	MYH9	P35579	226392	98	3
Myosin-9	MYH9	P35579	226392	96	1
Transitional endoplasmic reticulum ATPase	VCP	P55072	89266	64	4
78 kDa glucose-regulated protein	HSPA5	P11021	72288	35	2
78 kDa glucose-regulated protein	HSPA5	P11021	72288	81	4
Heat shock cognate 71 kDa protein	HSPA8	P11142	70854	21	2
Transforming growth factor-beta-induced protein ig-h3	TGFBI	Q15582	74634	232	11
Transforming growth factor-beta-induced protein ig-h3	TGFB1	Q15582	74634	195	6
Protein disulfide-isomerase	P4HB	P07237	57081	35	11
60 kDa heat shock protein, mitochondrial	HSPD1	P10809	61016	34	6
Protein disulfide-isomerase A3	ERP57	P30101	57081	156	6
Protein disulfide-isomerase A3	ERP57	P30101	57081	245	11
ATP synthase subunit alpha, mitochondrial	ATP5A1	P25705	59714	56	7
Vimentin	VIM	P08670	53619	97	9
Dolichyl-diphosphooligosaccharide-protein glycosyltransferase 48 kDa subunit	DDOST	P39656	50769	69	3
Tubulin alpha-1A chain	TUBA1A	Q71U36	50104	139	4
Tubulin beta-2C chain	TUBB2C	P68371	49799	105	4
Tubulin beta-2C chain	TUBB2C	P68371	49799	175	5
Ig gamma-1 chain C region	IGHG1	P01857	36083	107	6
Ig gamma-4 chain C region	IGHG4	P01861	35918	59	3